Continuous Process to Safely Manufacture an Aryldiazoacetate and its Direct Use in a Dirhodium-Catalyzed Enantioselective Cyclopropanation

Stephen P. Lathrop, Laurie B. Mlinar, Onkar N. Manjrekar, Yong Zhou, Kaid C. Harper, Eric R. Sacia, Molly Higgins, Andrew R. Bogdan, Zhe Wang, Steven M. Richter, Wei Gong, Eric A. Voight, Jeremy Henle, Moiz Diwan, Jeffrey M. Kallemeyn, Jack C. Sharland, Bo Wei and Huw M. L. Davies*

TOC FIGURE

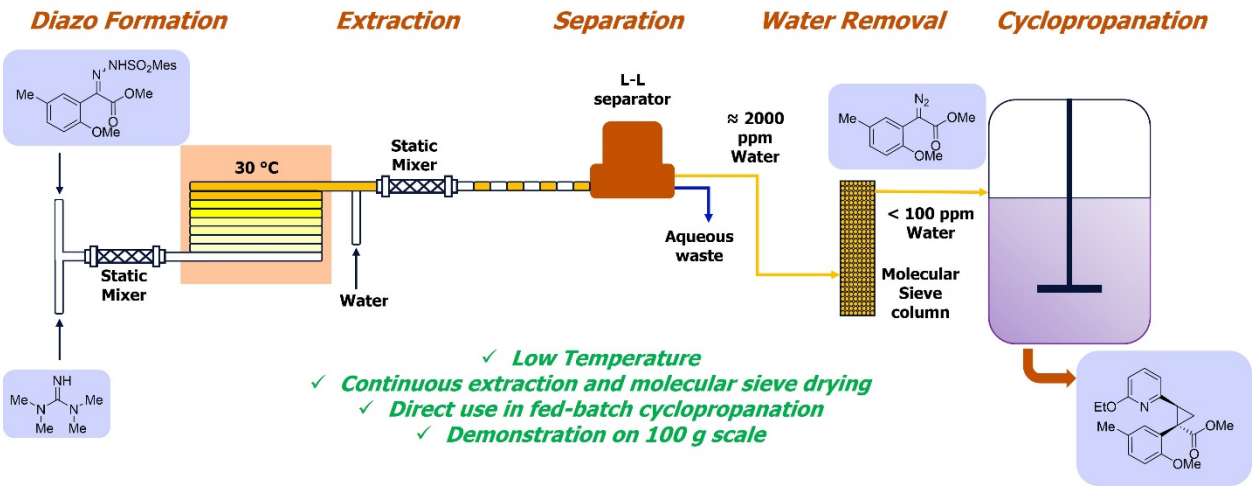

ABSTRACT

We report the development and demonstration of a continuous flow process for the safe formation, extraction and drying of aryldiazoacetate **2** which enables direct use in a fed-batch dirhodium catalyzed enantioselective cyclopropanation reaction to provide cyclopropane **4**. Designing this process with safety as a primary objective, we identified the appropriate arylsulfonyl hydrazone starting material and organic soluble base to facilitate a Bamford-Stevens diazo-generating flow process at 30 °C, well below the thermal onset temperature (T_{onset} = 57 °C), while also minimizing accumulation of the highly energetic diazo intermediate (ΔH_D = – 729 J/g). The Bamford-Stevens reaction byproducts are efficiently removed via a continuous aqueous extraction utilizing a liquid-liquid hydrophobic membrane separator. Continuous molecular sieve drying of the organic layer was demonstrated to maintain water levels <100 ppm in the final aryldiazoacetate solution, thereby ensuring acceptable reactivity, selectivity, and purity in the water sensitive cyclopropanation reaction. The full process was successfully executed on 100 g scale setting the foundation for the wider application of this and related chemistries on kilogram scale.

KEYWORDS: flow chemistry, aryldiazoacetate, continuous drying, cyclopropanation, process safety

INTRODUCTION

The synthetic utility of diazo compounds for the formation of a variety of unique and challenging chemical bonds is well appreciated.[1] Of these transformations, metal catalyzed reactions utilizing diazoacetates have been widely applied in the synthetic community to construct challenging C-C and C-heteroatom bonds via X-H (X = C,[2] N,[3] O,[4] S, P, Si[5]) insertion, cyclopropanation,[6] cycloaddition,[7] etc. However, one challenge that remains in the wider application of this chemistry for drug development is the danger associated with synthesis and use of these highly reactive diazo intermediates at scale.[8] Initiation of decomposition of diazoacetates can occur at temperatures as low as 60 °C resulting in significant exothermic events and nitrogen off-gassing.[9] This makes the synthesis and handling of these intermediates on large scale challenging. Concern regarding decomposition has limited their use in chemical and pharmaceutical manufacturing. Despite these challenges, a few examples of successful kilogram-scale synthesis and application of diazo intermediates have been demonstrated.[10] DelMonte and co-workers described the preparation of a styryldiazoacetate via diazo transfer in batch and its use in a metal-catalyzed cyclopropanation reaction for the kilogram-scale synthesis of HCV NS5B polymerase inhibitor beclabuvir.[10b] While the styryldiazoacetate prepared in this report had a relatively low thermal onset temperature (42 °C), the safety concern was partially mitigated via a fortuitous intramolecular electrocyclization that prevented nitrogen evolution. Similarly, Chen and co-workers conducted a kilogram-scale ruthenium catalyzed cyclopropanation using ethyl diazoacetate for the synthesis of a cyclopropyl indole containing serotonin reuptake inhibitor.[10a] Again, the diazoacetate was prepared in batch and used directly and although ethyl diazoacetate requires significant safety considerations, its preparation and use on scale has been well studied.[11] Additionally, Gage and co-workers described the rhodium

catalyzed intermolecular N-H insertion reaction of a diazoketoester on 100 kg scale using immobilized rhodium catalyst in flow for the synthesis of a carbapenem intermediate.[10c] However, the preparation and handling of the diazoketoester itself was not disclosed. These limited examples highlight the challenges and concerns associated with using these potentially explosive diazo intermediates on scale and underline the need for further investigation into methods for the safe large-scale preparation of these compounds.

Given the low onset temperatures for thermal decomposition and large energy of decomposition associated with diazoacetates, flow preparation of these intermediates has been utilized to allow for better heat control while minimizing the amount of diazoacetate formed at any given time. Previous examples of the flow preparation of diazoacetates[12] include, solid supported oxidation of hydrazones,[13] diazo transfer using sulfonyl azides,[14] and base-mediated elimination of aryl sulfonyl hydrazones (Bamford-Stevens reaction) (**Scheme 1**).[15] The oxidation of hydrazones using solid-supported metal oxidants offers the advantage of operating at ambient temperatures but can suffer from the use of stochiometric oxidants.[13a-g] This can lead to issues with leaching of oxidant into the product stream[13]**Error! Bookmark not defined.**[f,i,] and generates water as a byproduct which can interfere with downstream chemistry.[13h,i] Diazo transfer agents have also been exploited in the flow preparation of diazoacetates.[14] However, these azide-based diazo transfer reagents themselves are potentially explosive and must be synthesized and handled with care.[9] In contrast, arylsulfonyl hydrazones used in the Bamford-Stevens reaction have higher onset temperatures of decomposition and can be isolated as crystalline materials with good solid properties.[16] One drawback to the previously disclosed use of arylsulfonyl hydrazones for the preparation of diazoacetates in flow is the requirement for heating to ≥80 °C which is higher than the documented onset temperature of a number of

diazoacetates.**Error! Bookmark not defined.** Additionally, an inline silica column was required for the removal of the byproducts of the Bamford-Stevens reaction, namely triethylamine and the arylsulfinic acid.[15] In this work, we utilize a rationally designed substrate to allow for Bamford-Stevens reaction to operate at a reaction temperature below the onset temperature of decomposition of most diazoacetate products. We also demonstrate continuous aqueous extraction followed by molecular sieve column to remove reaction byproducts allowing for direct use of the diazoacetate solution in a water sensitive, highly enantioselective cyclopropanation reaction.

Scheme 1. General strategies for the flow preparation of diazoacetates.

A. Solid Phase Oxidation of Hydrazones

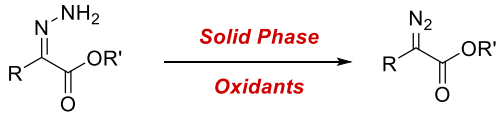

- water as byproduct - leaching of oxidant

B. Diazo Transfer

- preparation and handling of azide based reagent

C. Bamford-Stevens Reaction

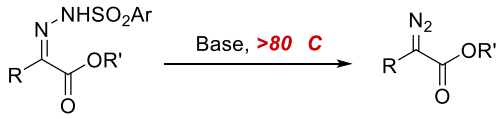

- high temperature - silica gel purification

D. *This Work:* Low temperature Bamford-Stevens Reaction

- low temperature
- continuous extraction and molecular seive drying
- direct use in fed-batch cyclopropanation
- demonstrated on 100 g scale

RESULTS AND DISCUSSION

Recently, a collaborative effort between AbbVie and the Davies group demonstrated the asymmetric rhodium-catalyzed cyclopropanation of vinyl heterocycles with a variety of aryl- and heteroaryl-diazoacetates.[17] This powerful transformation allows for the stereoselective synthesis of trisubstituted cyclopropanes containing a wide range of heterocyclic functionality. This new method was applied for the preparation of cyclopropane **4,** a relevant intermediate in the synthesis of a novel active pharmaceutical ingredient (API) (**Scheme 2**). To safely prepare gram quantities of intermediate **4** in batch mode, aryldiazoacetate **2** was prepared and its thermal stability assessed (*vide infra*). Due to a low onset temperature and tendency of neat diazo **2** to

exhibit exothermic crystallization, a crude solution of **2** in multiple smaller batches was employed in the key asymmetric cyclopropanation step. While these precautions were suitable for safe preparation of smaller quantities of cyclopropane **4**, flow chemistry was simultaneously assessed to enable larger scale reactions.

Scheme 2. Small scale batch synthesis of cyclopropane **4**.

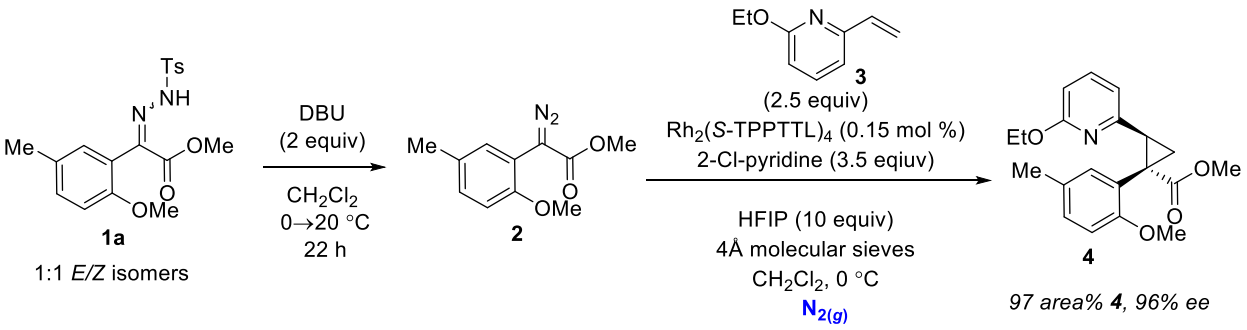

Challenges: low onset temperature of aryl diazoacetate **2** and water sensitivity of cyclopropanation reaction

To provide material for preclinical studies and in efforts to circumvent the safety issues related to the batch preparation and use of aryldiazoacetate **2**, a hybrid flow-fed-batch process similar to that described by Moody and co-workers[15] was developed for the preparation of cyclopropane **4** (**Figure 1**). It was found that treating tosyl hydrazone **1a** with 1,8-diazabicyclo(5.4.0)undec-7-ene (DBU) at 60 °C in flow could reduce a 12 h ambient batch process down to 10 min. In our initial flow setup, solutions of **1a** and DBU in anhydrous dichloromethane (DCM) were mixed at a tee-mixer using a Vapourtec E-Series and heated to 60 °C in a 10 mL PFA loop. A subsequent inline extraction was incorporated to remove water soluble byproducts (DBU and tolylsulfinic acid) using a static mixer and coupling the output with a Zaiput™ membrane separator (hydrophobic membrane). It was observed that using one volume of water in the extraction removed >90% of water-soluble byproducts. To purify further, a short silica gel column (pretreated with a solution of triethylamine) was coupled at the organic outlet of the membrane separator to remove any residual organic byproducts as well as water.

NMR analysis of the outlet stream following the silica gel column showed >95% purity aryldiazoacetate **2** (0.2 mmol/min at steady state). The outlet was collected in a vial containing molecular sieves and was shown to provide quantitative conversion to cyclopropane **4** when used in batch. Additionally, the outlet solution of aryldiazoacetate **2** could be fed directly into a round-bottom flask cooled to 0 °C containing the materials needed to facilitate conversion to **4**. Using this fed batch process, 4 g of cyclopropane **4** was isolated in 98% ee, which was used to prepare 5.43 g of API. This process allowed for the gram scale preparation of cyclopropane **4** while using only a 10 mL heated reactor coil, thus minimizing the amount of aryldiazoacetate **2** heated at any given time.

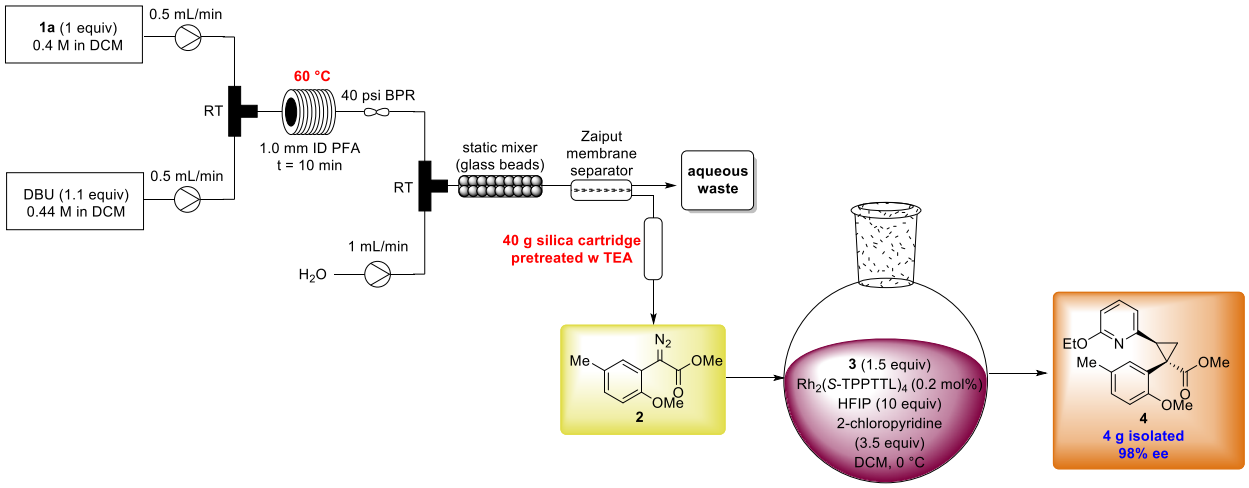

Figure 1. Proof-of-concept flow preparation of **2** and direct use in cyclopropanation reaction**.**

Although this proof-of-concept flow reactor allowed for the synthesis of gram quantities of cyclopropane **4**, there were several unanswered questions relating to the further scale-up of this reaction. Most notably, a significant safety concern with the stability of the aryldiazoacetate **2** would need to be further understood. Recently, a thorough study on the thermal stability of a variety of diazoacetates demonstrated that heating aryldiazoacetates as low as 61 °C can result in

significant exothermic events.[9] Therefore, understanding the safety window for the preparation and handling of aryldiazoacetate **2** is critical prior to further scale-up even when conducted in flow.

In addition to safety concerns associated with handling the aryldiazoacetate was the added challenge of the water sensitivity of the cyclopropanation reaction itself. The presence of water in the reaction has a twofold effect. First, if present in sufficient quantities, water can diminish the catalytic activity and enantioselectivity of the dirhodium catalyst. Second, in the presence of water and the rhodium catalyst, the aryldiazoacetate will undergo O–H insertion impacting both yield and product purity. Davies and co-workers found that hexafluoroisopropanol (HFIP) could be utilized as an additive to minimize the impact of water on the catalytic activity and enantioselectivity of the cyclopropanation reaction.[17] However, in the presence of water, HFIP fails to prevent the formation of the O–H insertion product, requiring the addition of a drying agent to maintain acceptable product yields.[13h] Therefore, we sought to develop a process for the safe and scalable formation and use of aryldiazoacetate **2** that addresses the safety concerns of the diazo intermediate and the water sensitivity of the cyclopropanation reaction. Herein we report a general strategy for the flow preparation, workup and drying of an aryldiazoacetate solution at a safe operating temperature enabling a continuous feed into a high yielding and highly stereoselective cyclopropanation reaction amenable for further scale-up. We believe the strategy employed here is general and should be easily adaptable for transformations requiring the safe handling of sensitive aryldiazoacetates under "anhydrous" conditions.

A differential scanning calorimeter (DSC) and an accelerating rate calorimeter (ARC) were used to understand appropriate operating temperatures and safety considerations for the

handling of aryldiazoacetate **2**. DSC was used to determine the enthalpy of decomposition (ΔH_D), which indicates the energetic yield of the decomposition, as well as the initiation temperature (T_{init}), which is defined here as the beginning of the exothermic decomposition peak as monitored by DSC.[18] Initial DSC testing provided insight into the thermal stability of the compound and its potential prevalence for runaway reactions upon scale-up. DSC analysis of aryldiazoacetate **2** showed the initiation temperature to be 65 °C with a ΔH_D of – 729 J/g (**Figure 2**). It should be noted that the proximity of the endothermic peak associated with melting of the aryldiazoacetate **2**, to the exothermic feature associated with decomposition can introduce increased error in precise assignment of T_{init}.

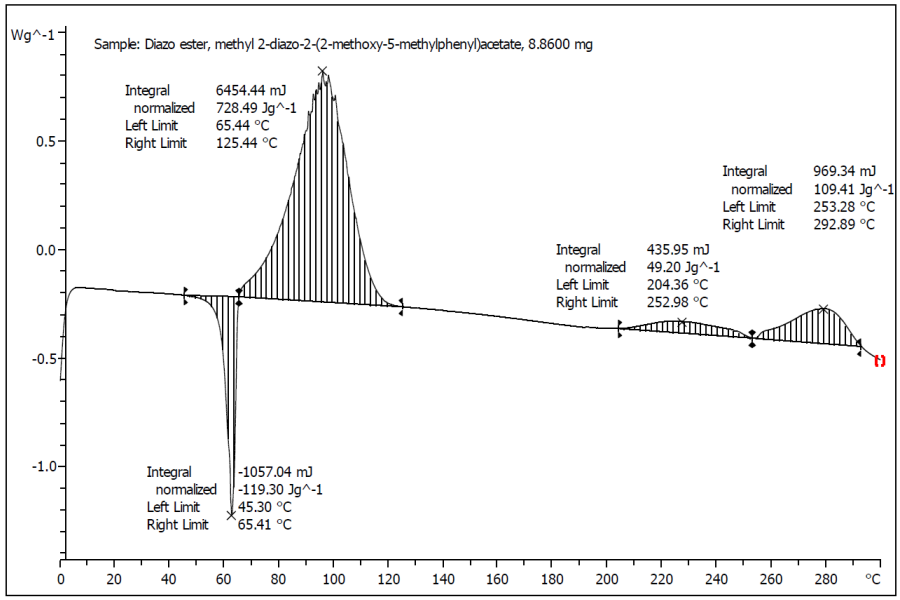

Figure 2. DSC of aryldiazoacetate **2**

The DSC data is consistent with literature examples showing that aryldiazoacetates substituted with an electron rich aromatic ring have lower initiation temperatures than electron neutral or deficient counterparts (**Table 1**).[9] Additionally, more sensitive ARC experiments with the aryldiazoacetate forming Bamford-Stevens post-reaction mixture detected significant exothermic

events at 52 °C and 198 °C resulting in adiabatic temperature rises (ATR) of 36 °C and >164 °C respectively. The exothermic event detected at 52°C is likely due to the decomposition of formed aryldiazoacetate **2** and resulted in ~ 1 equiv of gas evolution (presumably nitrogen).

Table 1. Thermal stability and exotherm data of representative aryldiazoacetates.

Entry	Compound	Structure	R	T_{init} (°C)[a]	ΔH_D (J g^{-1})
1	**2**	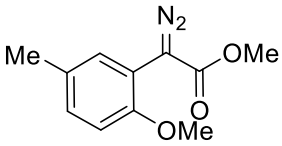	--	65	–730
2[b]	**5a**		2-MeO	61	–521
3[b]	**5b**	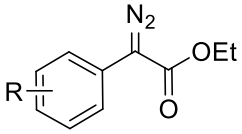	H	87	–539
4[b]	**5c**		2-CF_3	79	–407
5[b]	**5d**		4-NO_2	113	–578

[a]Measured by DSC. [b]Obtained from Ref **Error! Bookmark not defined.**

Due to the diminished heat transfer area of jacketed batch reactors per unit volume upon scale-up, substantial safety measures are routinely applied when scaling exothermic reactions, especially reactions that generate gas during decomposition.[19] For this reason, the significantly improved heat transfer capabilities of flow reactors provide a preferred method to de-risk chemistries that are prone to exothermic reactions and decomposition. Furthermore, flow reactors provide the advantage of minimizing the quantity of the potentially energetic intermediate that is generated at any one time. A conservative assessment of the explosive propagation potential using the Pfizer-modified Yoshida correlation[20] for compound **2** and the T_{init} and ΔH_D from **Table 1** provides a value ≥ 0, indicating the isolated molecule has the potential to be explosive. This finding further reinforces the inherent importance of safety considerations in the process design during scale-up. Though not always sufficient depending on the specific

case, a common industry practice suggests a 50 °C safety buffer between onset and target temperature in batch when measured with accelerating rate calorimeter (ARC) and even larger buffers if using DSC to determine the T_{onset}.[21] ARC studies for a representative reaction mixture showed a > 0.02°C/min self-heating rate, indicating onset of decomposition of **2**, beginning at 52 °C. Therefore, to safely scale this reaction in a batch configuration would require maintaining an internal temperature of 2 °C or less during all unit operations, which is less preferred due to the slower rate of formation of aryldiazoacetate at these temperatures. Additionally, we sought to minimize the handling and accumulation of this sensitive and hazardous intermediate. Because of this, flow was pursued as a strategy for the scale-up preparation of aryldiazoacetate **2**.

To enable a safe, scalable flow chemistry approach, reaction optimization and kinetic analysis were performed on the Bamford-Stevens reaction to generate aryldiazoacetate **2**. Previously, this transformation was either conducted at high temperatures (≥60 °C) in a plug flow reactor for short reaction times or at ambient temperature in batch, requiring more than 12 h to reach completion. Neither of these options were deemed appropriate for scale-up of the process due to the unsafe operating temperature and the accumulated quantity of diazoacetate, respectively. Therefore, a change to the reaction conditions and/or reagents was required with the goal of increasing the reaction rate and lowering the reaction temperature well below the onset temperature for decomposition of the aryldiazoacetate **2** solution (52 °C). The tosyl hydrazone **1a** was initially selected as the substrate and a variety of bases were examined in the Bamford-Stevens reaction of this hydrazone to evaluate the effect on reaction rate (**Table 2**, entries 1-5).[22] Reactions were conducted in dichloromethane (DCM) at 38 °C and the time to reach 95% conversion was determined for each base by HPLC monitoring. Not surprisingly, stronger bases resulted in more rapid hydrazone decomposition to provide the desired

aryldiazoacetate **2**. However, based on these data, conducting the reaction at 38 °C even with 2-*tert*-butyl-1,1,3,3-tetramethylguanidine (BTMG, Barton's base) would require 40 min to reach 95% conversion (entry 5). These conditions would not lend themselves to development of an ideal flow process.

Table 2. Bamford-Stevens Reaction Screen.

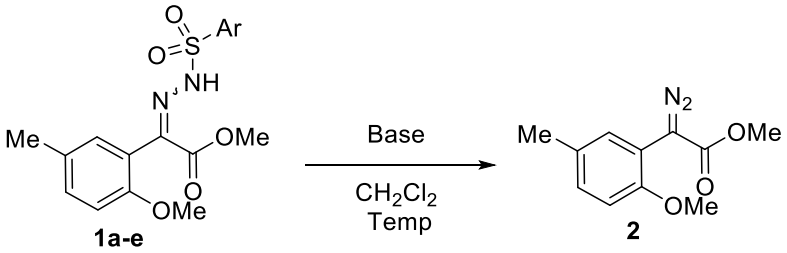

Entry	Ar	Isomeric ratio (*E/Z*)[b]	Base	Temp (°C)	Time to 95% Conv (min)[c]
1	4-MePh, **1a**	50:50	DBU	38	105
2	4-MePh, **1a**	50:50	TBD	38	110
3	4-MePh, **1a**	50:50	TMG	38	120
4	4-MePh, **1a**	50:50	TEA	38	230
5	4-MePh, **1a**	50:50	BTMG	38	40
6	Ph, **1b**	75:25	BTMG	38	30
7	2,4,6-iPrPh,1**c**	61:39	BTMG	38	2.5
8	2-NO_2Ph, **1d**	55:45	BTMG	38	15
9	2,4,6-MePh, **1e**	77:23	BTMG	38	5
10	2,4,6-MePh, **1e**	77:23	BTMG	30	6
11	2,4,6-MePh, **1e**	77:23	TMG	30	9
12	2,4,6-MePh, **1e**	77:23	DBU	30	12

[a]Conditions: **1a-e** (1 equiv), base (1.2 equiv), CH_2Cl_2 (10V). [b]Determined by ^{1}H NMR. [c]Time to reach 95% conversion of **1a-e**; DBU = 1,8-diazabicyclo(5.4.0)undec-7-ene, TBD = 1,5,7-triazabicyclo[4.4.0]dec-5-ene, TMG = 1,1,3,3-tetramethylguanidine, TEA = triethylamine, BTMG = 2-*tert*-butyl-1,1,3,3-tetramethylguanidine or Barton's base.

Previous literature data has shown that changing the identity of the aryl group of the sulfonyl hydrazone has direct impact on the rate of elimination.[15a,23] With this in mind, a variety of

differentially substituted aryl sulfonyl hydrazones were evaluated in the Bamford-Stevens reaction with Barton's base (**Table 2**, entries 6-9). Indeed, changing the identity of the sulfonyl hydrazone significantly impacted the reaction rate, with triisopropylbenzenesulfonyl hydrazone **1c** providing 95% conversion in 2.5 min (entry 7). However, triisopropylbenzenesulfonyl hydrazone **1c** required a custom sulfonyl hydrazide, and the isolation and purification of the corresponding hydrazone **1c** was challenging. In comparison, the mesitylsulfonyl hydrazone **1e** provided high conversion in 5 min (entry 9). In contrast to hydrazone **1c**, the mesitylsulfonyl hydrazone **1e** could be easily prepared from commercial materials and directly isolated as a crystalline solid in high purity. Use of benzenesulfonyl hydrazone **1b** and 2-nitrobenzenesulfonyl hydrazone **1d** did not provide significant improvement in reaction rate (entries 6 and 8). Due to these considerations, a concession in terms of throughput was necessary, and the decision to further optimize the elimination reaction with mesitylsuflonyl hydrazone **1e** was made.

To maximize reaction rate while minimizing reaction temperature, a base screen was conducted with the mesitylsulfonyl hydrazone **1e** at 30 °C. Again, a direct correlation to the strength of the base and reaction rate was observed (**Table 2**, entries 10-12). Use of BTMG provided 95% conversion in 6 min (entry 10) while 1,1,3,3-tetramethylguanidine (TMG) provided the same conversion in 9 min (entry 11) and 1,8-diazabicyclo(5.4.0)undec-7-ene (DBU) required 12 min to obtain similar conversion (entry 12). Due to cost and material availability considerations along with knowledge that nearly complete rejection of TMG could be achieved using a single water wash (*vide infra*), TMG was chosen as the base for further development.

To ensure the newly optimized reaction conditions were appropriate for further scale up, additional safety studies were carried out with hydrazone **1e** and TMG. Using an Omnical

SuperCRC (Chemical Reactivity Calorimeter), it was determined that the addition of TMG to hydrazone **1e** was exothermic resulting in a 15 °C ATR. Additionally, the onset temperature of the reaction mixture was again measured using ARC and determined to be 57 °C, which was comparable to the previous reaction using tosyl hydrazone **1a** and DBU. Given the calorimetric data and the targeted reaction temperature of 30 °C, we determined these flow conditions were amenable for further scale up with minimal risk of reaching the onset temperature of the aryldiazoacetate reaction mixture.

Following optimization of the batch reaction conditions, development of the aryldiazoacetate flow reaction was undertaken. Use of a flow reaction for formation of the aryldiazoacetate affords the ability to provide improved heat control through a high surface area to volume ratio. The accumulation of the aryldiazoacetate within the reactor system was also well-controlled using a semi-continuous process whereby a flow reaction to form the aryldiazoacetate is effectively quenched into a fed-batch cyclopropanation reaction at low temperature (*vide infra*). Further evaluation of the reaction kinetics of the diazo ester formation reaction in batch revealed >99% conversion of the mesitylsulfonyl hydrazone **1e** in 15 min at 30 °C with TMG as the base (**Figure 3**). Based on these results a 15 min residence time for a flow reaction was targeted.

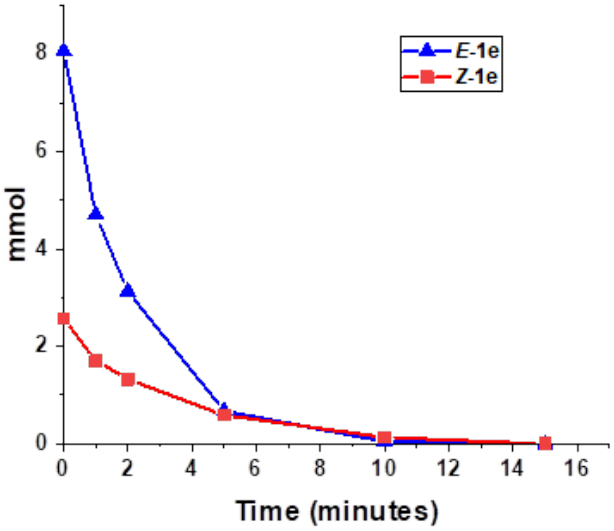

Figure 3. Conversion of mesitylsulfonyl hydrazone **1e** at 30 °C with TMG in DCM.

The reaction conditions and homogeneous nature of the system led to design of a plug flow reactor (PFR). For lab studies, a PFR with a 1/8" OD (1/16" ID) was designed. Two streams were mixed through the incorporation of a static mixer. As shown in **Figure 4**, stream A consisted of mesitylsulfonyl hydrazone **1e** in dichloromethane (DCM) at a target concentration of 0.76 M. Stream B was composed of 1.1 equiv. of TMG in DCM at a target concentration of 0.83 M. The overall process volume of 5 to 5.5 mL/g was selected to minimize solvent use while ensuring complete dissolution of the hydrazone starting material. At the 1/16" ID scale, 0.2 mL/min flow rates were selected for each input stream utilizing a Syrris Asia syringe pump. Flow rates selected were verified to result in laminar flow through calculation of the Reynolds number (Re < 100). The flow process was designed to be executed in a laminar flow regime, which guided the calculations and design of the large-scale process. The PFR internal temperature was maintained at 30 °C utilizing a water bath for temperature control.

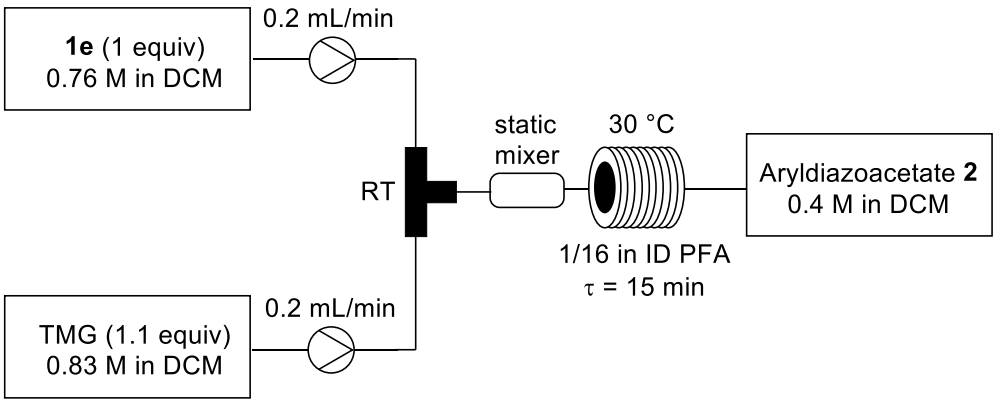

Figure 4. PFR design for preparation of aryldiazoacetate **2**.

Steady state operation of the PFR was verified through incorporation of an IR flow cell. IR results showed that steady state was achieved after ~2 residence times (**Figure 5**). Offline analysis by qNMR showed 5.6 wt% of diazo ester at steady state operation corresponding to a 90% yield of **2**. Based on these results we were confident that the flow reactor described above would be sufficient to consistently deliver aryldiazoacetate **1e** at a reaction temperature well below the onset temperature (57 °C).

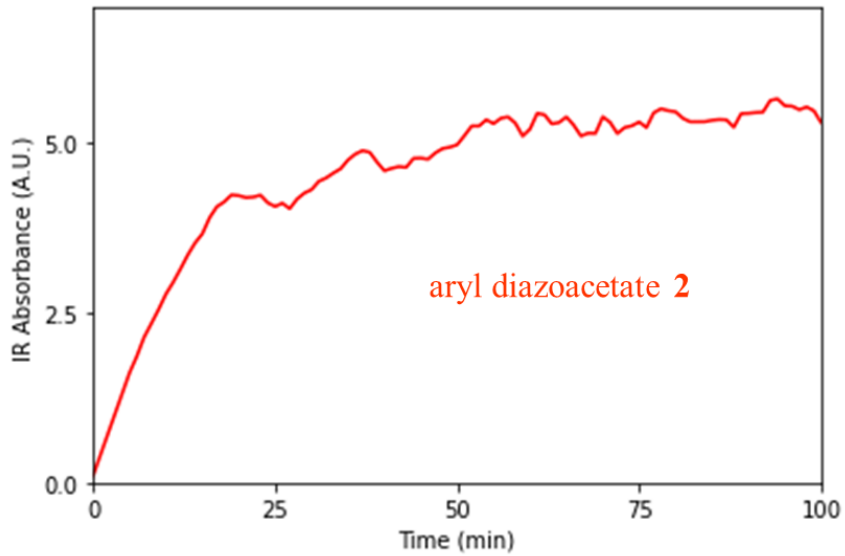

Figure 5. React IR trace for PFR aryldiazoacetate formation

Having developed a PFR for the safe formation of aryldiazoacetate **2,** our focus turned to removal of the reaction byproducts of excess TMG and the mesitylsulfinic acid TMG salt. It was determined that using the crude aryldiazoacetate stream in the cyclopropanation reaction without removal of TMG and mesitylsulfinic acid TMG salt resulted in slower conversion and an increase in impurity formation. Additionally, the ee of **4** improved from 94% to 98% when TMG and mesitylsulfinic acid TMG salt were removed prior to the cyclopropanation reaction. These results are consistent with previous observations that Lewis basic additives can alter catalytic activity of similar dirhodium catalysts.[17,24] After evaluating our options, we determined that an aqueous extraction provided the best approach to remove both TMG and the mesitylsulfinic acid TMG salt efficiently and safely prior to the cyclopropanation reaction. To significantly limit the holdup of aryldiazoacetate **2**, a continuous extraction process was designed. Water was selected as the extraction solvent based upon the ability to remove both TMG and the mesitylsulfinic acid TMG salt. As part of the flow reactor design, water was introduced through a tee junction, immediately following the PFR, with an inline static mixer inserted to effectively mix the aqueous wash and organic product stream. While a mixer settler setup was first considered, a desire to minimize aryldiazoacetate accumulation and hold up led to the selection of a membrane-based separation.[25] Membrane separators have the advantage of minimizing reactor hold up and can efficiently separate aqueous and organic streams. For this process, a Zaiput™ equipped with 1 μm hydrophobic PTFE membrane was utilized. As illustrated in **Figure 6a**, efficient partitioning can be easily visualized by the separation of the colorless aqueous and the yellow product-containing organic layer.

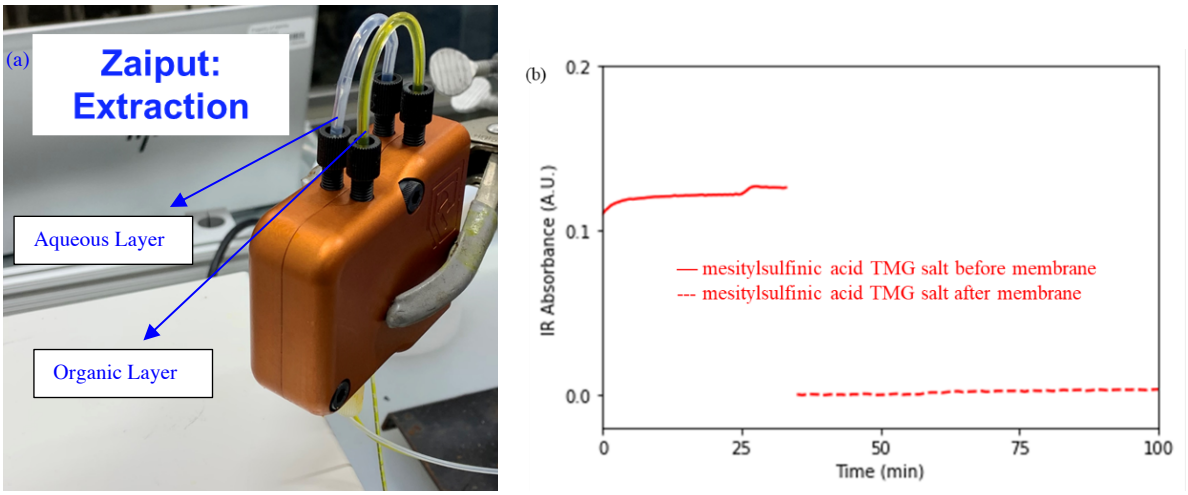

Figure 6. (a) Zaiput membrane extractor. (b) IR of mesitylsulfinic acid TMG salt in organic layer before and after Zaiput membrane separator.

The efficiency of the separation was further confirmed by analyzing losses of the aryldiazoacetate **2** to the aqueous layer which were typically < 3% and measuring the water content of the DCM layer which was typically ~ 1500 ppm, consistent with water-saturated DCM. During small development runs the TMG and the mesitylsulfinic acid TMG salt content were monitored in the organic layer after the Zaiput membrane separation by both inline IR and offline qNMR analysis. The inline IR showed only low levels of the mesitylsulfinic acid TMG salt in the organic layer while TMG was unable to be monitored by IR due to signal overlap (**Figure 6b**). The qNMR data for the removal of the mesitylsulfinic acid TMG salt was consistent with IR data and was maintained below <0.05 wt%. qNMR also showed that TMG was well rejected to the aqueous layer with ≤0.1 wt% being observed in the organic layer throughout the run (**Table 3**). Spiking studies showed that up to 1 wt% of TMG and mesitylsulfinic acid each were well tolerated in the cyclopropanation reaction.[26] These results highlight the efficiency of the membrane separator to effectively separate the aqueous and

organic layers, minimizing the accumulation of aryldiazoacetate solution while providing effective removal of TMG and the mesitylsulfinic acid TMG salt from the organic stream.

Table 3. Efficiency of Aqueous Extraction.

Time (min)	wt% TMG[a]	wt% mesitylsulfinic acid TMG salt[a]
0[b]	3.6	3.7
15	0.08	0.02
32	0.08	0.02
82	0.10	0.03

[a]Weight percent measured in organic layer by ^{1}H qNMR. [b]Organic layer prior to aqueous extraction.

Having identified a method for efficient removal of reaction byproducts via a continuous extraction we next sought to further understand if the purified aryldiazoacetate solution could be used directly in the cyclopropanation reaction. In the design of our overall process, we envisioned the aryldiazoacetate product stream being added to a batch reactor containing the vinyl pyridine **3** and the dirhodium catalyst.[27] However, after continuous extraction the aryldiazoacetate solution contained ~1500 ppm water. Due to the known sensitivity of the cyclopropanation reaction to water, it was necessary to further understand the impact of water on the cyclopropanation reaction purity and enantioselectivity. Additionally, due to the large energy of decomposition associated with aryldiazoacetate **2** (ΔH_D = –729 J/g) it was desirable to minimize accumulation of the aryldiazoacetate **2** in the cyclopropanation reaction. Therefore, it was critical to also understand the impact of water on the rate and conversion of the cyclopropanation reaction.

Table 4. Water Spiking Studies on Cyclopropanation Reaction[a]

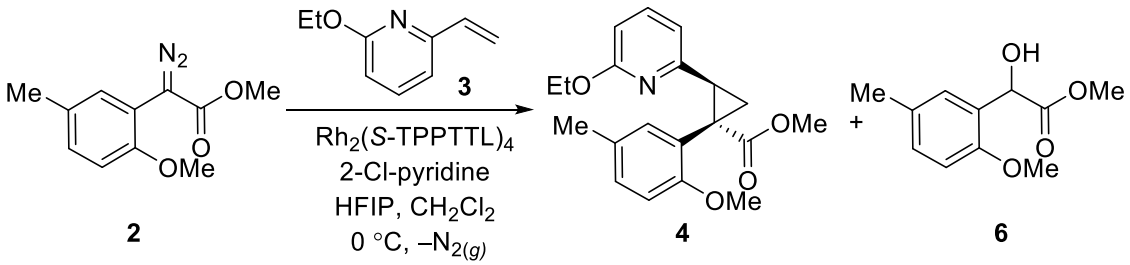

Entry	Equiv Water	Nitrogen Sparge?	Time (h)	% **2** remaining	Area% **4**	Area% **6**	%ee **4**
1[b]	0.04	No	1	0	97	0.6	96
2	0.15	No	1	0	90	6	98
3	0.34	No	22	47	30	16	n/a
4	0.46	No	28	69	18	14	n/a
5	0.34	Yes	1	0	70	25	98
6	0.46	Yes	1	1	73	22	98

[a]Conditions: **2** (0.454 mmol, 1 equiv), **3** (0.681 mmol, 1.50 equiv), Rh_2(*S*-TPPTTL)$_4$ (0.681 μmol, 1.5 mol %), 2-Cl-pyridine (1.59 mmol, 3.50 equiv), HFIP (4.54 mmol, 10.0 equiv), CH_2Cl_2 (20V), 0 °C. [b]Dried over 500 wt% 4Å molecular sieves.

To further refine our understanding on the impact of water in this reaction a series of water spiking experiments were conducted (**Table 4**). As highlighted in **Scheme 2** and recapitulated in **Table 4**, entry 1, running the reaction in the presence of molecular sieves results in complete conversion and high area% purity of the desired cyclopropane **4** in good ee. The addition of water, 0.15 equivalents, still results in complete consumption of aryldiazoacetate **2** in 1 h, however, 6 area% of the corresponding O–H insertion product **6** is observed along with a corresponding drop in the overall purity of cyclopropane **4** (entry 2). Encouragingly, the presence of water had no impact on the enantioselectivity, and the product was obtained in 98% ee. This result is consistent with Davies and co-workers' observation that the presence of HFIP minimizes the negative impact of water on the enantioselectivity of the cyclopropanation reaction.[17] Increasing the water content to 0.34 equivalents results in incomplete reaction

conversion and significant formation of **6** (entry 3). Further increasing the amount of water to 0.46 equivalents exacerbates this effect and 69% unreacted aryldiazoacetate remains after 28 h (entry 4). Based on empirical observations that bubbling nitrogen through the reaction mixture prior to addition of the aryldiazoacetate resulted in accelerated reaction rates, the effect of nitrogen sparging was examined in the presence of water. When the conditions implemented in entries 3 and 4 were repeated with inclusion of nitrogen sparging of the reaction mixture prior to addition of the aryldiazoacetate solution, complete conversion was observed, and the product was obtained in 98% ee (entries 5 and 6). As expected in these examples with elevated water spiked, increased levels of the O–H insertion product **6** were observed. However, these results provided confidence that the reaction can tolerate low levels of water without impacting reaction conversion or enantioselectivity. The lack of impact on conversion had significant implications to our proposed fed batch flow reactor design and provided confidence that accumulation of the aryldiazoacetate in the cyclopropanation reaction could be minimized by appropriate control of water. Based on these water spiking studies and the tolerance for **6** downstream, we sought to target a water content of <100 ppm (~0.03 equiv) in the cyclopropanation reaction.

To determine the optimal method for water removal the drying capacity of silica gel and 5 different types of molecular sieves were evaluated in a batch study. Water saturated DCM containing ~1500 ppm water was treated with the desiccants and the water content of the DCM was monitored over 6 days (**Table 5**). Compared to molecular sieves and consistent with previous reports,[28] silica was found to be less efficient at removing water than the molecular sieves examined (entry 1). However, all five molecular sieves evaluated showed equal capacity for water removal (entries 2-6).

Table 5. Batch drying of wet dichloromethane with desiccants.

Entry	Desiccant	Absorption (g water absorbed/kg of desiccant)		
		1 day[a]	3 days[a]	6 days[a]
1	Silica Gel	20.9	20.6	n/a
2	3Å spherical molecular sieves	31.4	32.9	33.9
3	4Å powdered molecular sieves	32.8	33.9	33.4
4	5Å spherical molecular sieves	32.2	33.4	33.8
5	4Å spherical molecular sieves	30.7	32.1	33.4
6	3Å pellet[b] molecular sieves	30.9	31.0	31.0

[a]Time exposed to water scavenger. [b]Extruded cylinder

Although it has been demonstrated that the addition of molecular sieves to the cyclopropanation reaction works well on gram scale to mitigate the impact of water on the reaction, the practicality of an in-situ heterogeneous drying step diminishes as scale increases due to considerations such as: possible etching of glass reactors, slow filtration associated with removal of powdered molecular sieves, and ensuring removal of the molecular sieves between batches in large scale equipment. Therefore, we sought to test the performance of the desiccants in continuous mode, by comparing performance of molecular sieves in a packed column. Three desiccants were tested in a packed 2.5 cm diameter column and water saturated DCM was fed through the column at 12 mL/min in up flow. The water content of the DCM output solution was measured and plotted against water saturated DCM passed through the column per gram of desiccant. The results are highlighted in **Figure 7**. Performance of the 3Å molecular sieves was

superior to both 4Å and 5Å and was selected for scale up. Based on the data obtained in **Figure 7**, 26 L of water saturated DCM could be processed per kg of 3Å molecular sieves while maintaining output water content below the target of 100 ppm. Given our expected output stream concentration of 0.4 M, we anticipated being able to process 4.2 kg of hydrazone **1e**/kg of molecular sieves.

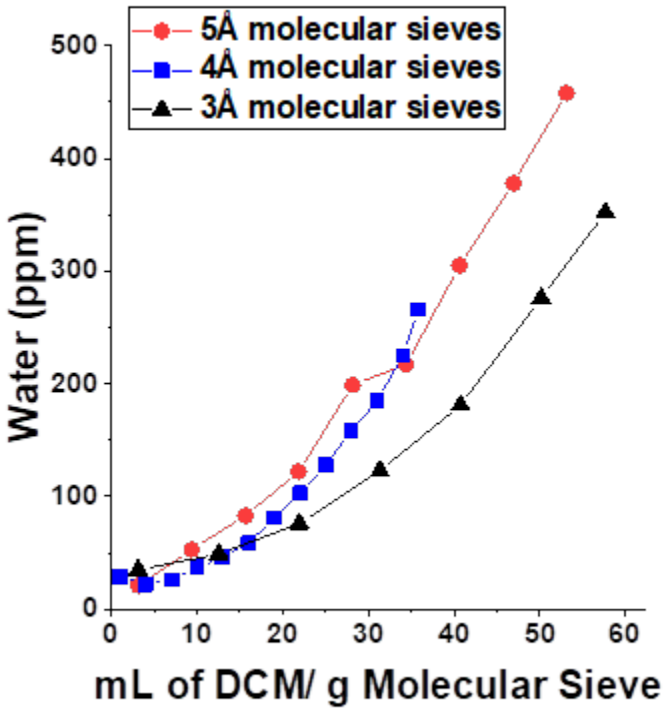

Figure 7. Packed bed molecular sieve drying of saturated dichloromethane solution showing 3Å molecular sieves provide the highest capacity for water removal.

Having identified a method for the removal of water below the target of 100 ppm we sought to further understand the impact of changing the equivalents of HFIP and 2-chloropyridine on the cyclopropanation reaction in the presence of 0.15 equivalents of water (**Table 6**). It was determined that lowering the equivalents of HFIP from 10 to 5 resulted in a

lower enantioselectivity of 93% ee (entry 2); while further lowering the equivalents of HFIP to 2.5 resulted in only 41% reaction conversion (entry 3). These results are consistent with previous work showing that poor conversion and enantioselectivity are observed in the presence of water and in the absence of molecular sieves or HFIP.[17] The equiv of 2-chloropyridine were then examined and to our delight the equiv could be lowered to 1.0 without impacting reaction conversion or enantioselectivity (entries 4 and 5). However, lowering to 0.5 equiv of 2-chloropyrdine results in lower 95% ee (entry 6).[29] Finally, due to challenges removing 2-chloropyridine downstream and data suggesting 2-chloropyridine is a genotoxic impurity,[30] 2-fluoropyridine was evaluated as an additive in the reaction. Consistent with work published by Davies and co-workers, 2-fluoropyridine provides essentially the same results as 2-chloropyridine and can be easily removed downstream via solvent swap distillation. Based on these studies, conducting the reaction with 10 equiv of HFIP and 1.1 equiv of 2-fluoropyridine was pursued for scale up of the planned fed-batch cyclopropanation reaction.

Table 6. HFIP and 2-Halopyridine Ranging Studies[a]

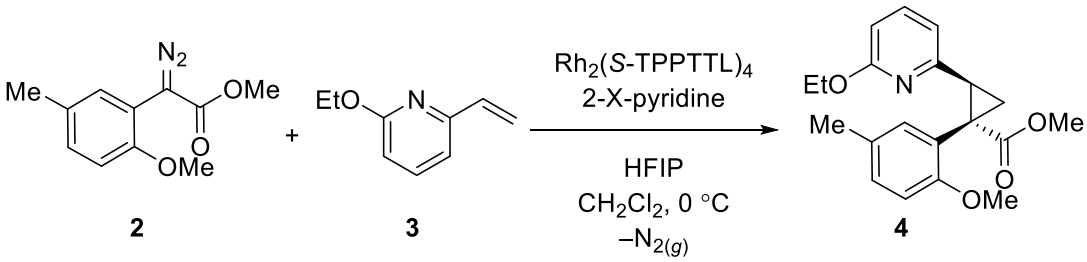

2 **3** **4**

Entry	X=	Equiv HFIP	Equiv 2-X-pyr	%Conversion	%ee
1	Cl	10	3.5	100	98
2	Cl	5	3.5	99	93
3	Cl	2.5	3.5	41	n/a
4	Cl	10	2.5	100	98
5	Cl	10	1.0	100	98
6	Cl	10	0.5	99	95
7	F	10	1.1	100	98

[a]Conditions: **2** (0.454 mmol, 1 equiv), **3** (0.590 mmol, 1.30 equiv), Rh_2(*S*-TPPTTL)$_4$ (0.681 μmol, 1.5 mol %), 2-X-pyridine, HFIP, CH_2Cl_2 (20V), 0 °C.

Additional studies were also performed to assess the cyclopropanation reaction performance in an OmniCal SuperCRC calorimeter equipped with a mass flowmeter to measure the reactor off gas flowrate. Measurement of N_2 gas generation during the experiment demonstrated that the selective cyclopropanation reaction displays an apparent first order dependence on both the aryldiazoacetate **2** and the vinyl pyridine **3**.[26] At 2 °C, the batch reaction was 50% complete in 1.4 min and 95% complete in 9.0 min. The overall second order dependence on the two reactants further supported the choice of a fed-batch configuration to limit the accumulation of the aryldiazoacetate **2** using excess vinyl pyridine **3** to minimize accumulation.

Having studied each element of the planned process independently we sought to demonstrate scale-up of a fully continuous aryldiazoacetate formation reaction, aqueous

extraction, and water removal, followed by a fed-batch cyclopropanation reaction. The fully continuous process was performed utilizing 100 g of hydrazone **1e** to ensure steady state conditions could be achieved with the detailed reactor design and to determine throughput for anticipated larger scale campaigns. The process flow diagram for the demonstration batch is shown in **Figure 8a**. The design centers on the synthesis of the aryldiazoacetate via PFR at 30 °C using 1/8" tubing and 1.1 mL/min flow rate for each reagent/starting material solution resulting in a 15 min residence time. Once complete, the aryldiazoacetate stream is combined with water at a rate of 2.2 mL/min and passed through a static mixer to facilitate removal of excess TMG and the mesitylsulfinic acid TMG salt from the organic layer. The biphasic mixture is then separated using the Zaiput™ membrane filtration system described previously. The resulting organic layer, containing aryldiazoacetate **2** and ~1500 ppm water, is then passed through a 2.5 cm diameter column packed with 3Å molecular sieve (105 g, height of the molecular sieve bed is 25 cm). Based on breakthrough experiments highlighted in **Figure 7**, 105 g of molecular sieves is expected to process 2.5 L of water saturated dichloromethane maintaining output concentration below 100 ppm corresponding to ~400 g of hydrazone input. The resulting dried organic stream is then added to a jacketed reactor containing a solution of dirhodium catalyst, vinyl pyridine **3**, HFIP and 2-fluoropyridine in DCM cooled to 0 °C. To ensure catalyst performance and minimize impurity formation the solution of vinyl pyridine, 2-fluoropyridine and HFIP in DCM is also dried through a 3Å molecular sieve column (2.5 cm diameter, 50 g of molecular sieve) prior to use.

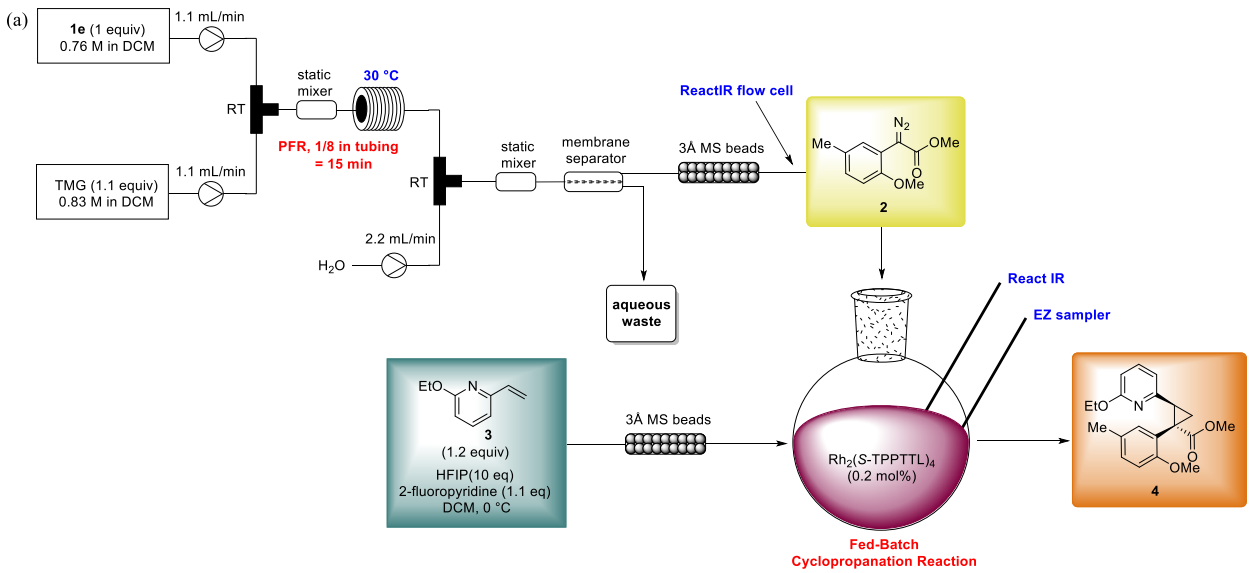

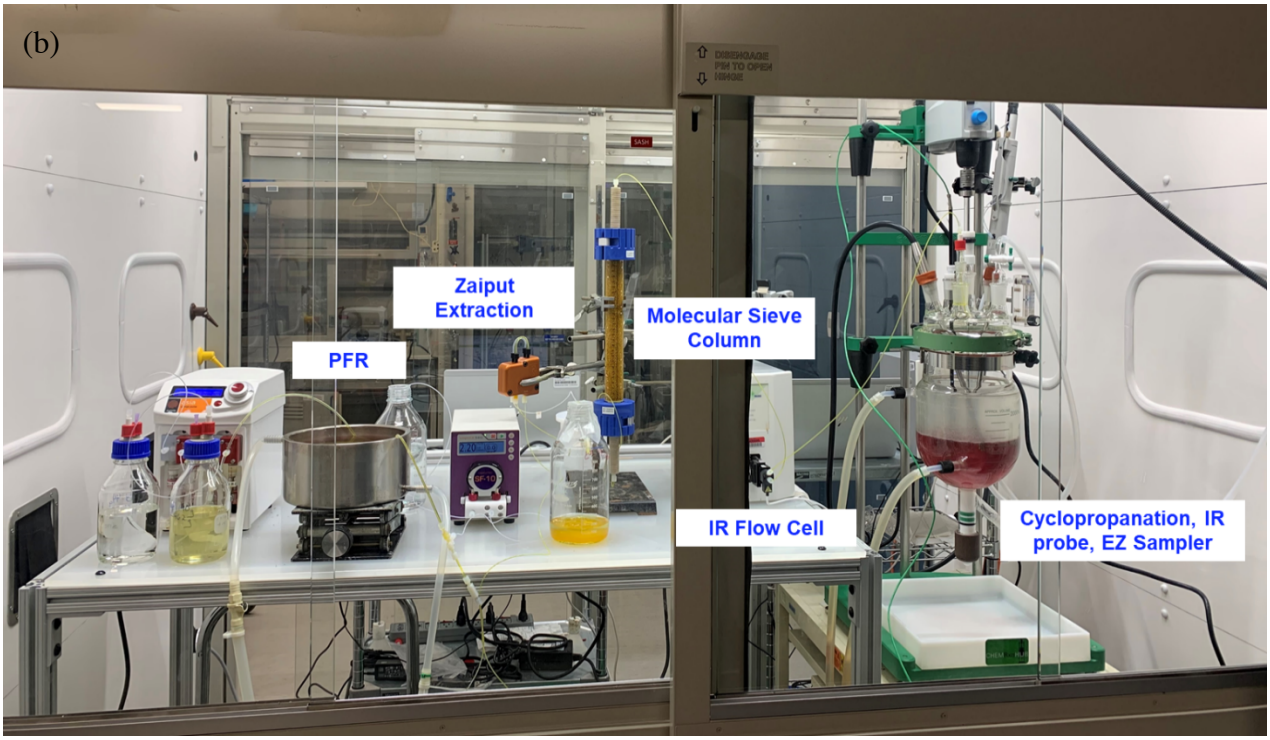

Figure 8. (**a**) Schematic of flow reactor design (**b**) Flow reactor setup for 100 g demonstration.

Critical to the design of the flow process was the implementation of react IR to monitor both the formation of aryldiazoacetate **2** and the cyclopropanation reaction in real time. As shown in **Figure 9**, the addition of the aryldiazoacetate **2** to the cyclopropanation reaction was

started after the equivalent of approximately three residence times through the complete flow system.[31] At steady state (~ 150 min) the concentration of the aryldiazoacetate solution was determined to be 6.2 wt% by offline qNMR analysis, corresponding to 90% yield of aryldiazoacetate **2**. The performance of the phase separation was assessed by qNMR and consistent with smaller scale runs <0.1 wt% TMG and mesitylsulfinic acid TMG salt was observed in the organic stream. Water content of the aryldiazoacetate stream after the molecular sieve column was measured periodically by Karl-Fisher analysis and remained less than 100 ppm throughout the course of the reaction, in line with expectations.

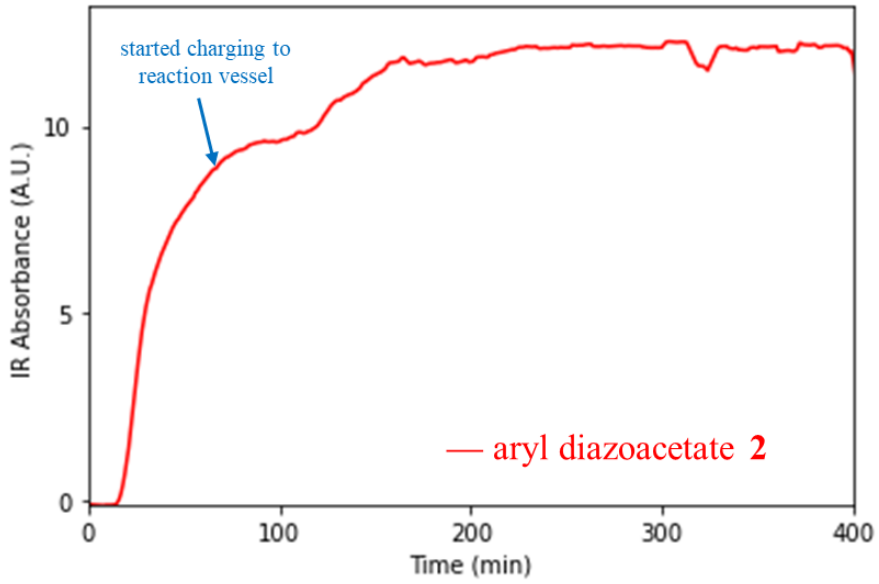

Figure 9. IR analysis of diazoacetate formation in PFR.

Monitoring the cyclopropanation reaction by react IR ensured consistent conversion to cyclopropane **4** while also confirming minimal accumulation of the aryldiazoacetate **2**. In the event of aryldiazoacetate **2** accumulation due to catalyst inactivity the flow reactor could be safely shut down by diverting the flow of the diazo containing product stream to a quench reactor containing methanolic phosphoric acid. The IR results from the cyclopropanation reaction are

shown in **Figure 10** and confirm consistent formation of the desired cyclopropane **4** along with consumption of the vinyl pyridine **3**. Importantly, no significant accumulation of the aryldiazoacetate **2** was observed. In addition to react IR monitoring, the cyclopropanation was monitored via automated sampling and offline HPLC analysis. HPLC analysis showed consistent results with the react IR and aryldiazoacetate **2** was maintained below 0.07 wt% throughout the reaction (**Figure 10b**). Overall, the aryldiazoacetate solution was added to the batch reactor for 20 turnovers of the PFR reactor (300 min), corresponding to 100 g of hydrazone and resulting in 74% assay yield,[32] 93 area% purity and 98% ee of the desired cyclopropane **4**. Importantly, the O–H-insertion product **6** was observed in only 7% assay yield (2.5 area%) and was well within tolerated levels for downstream chemistry.

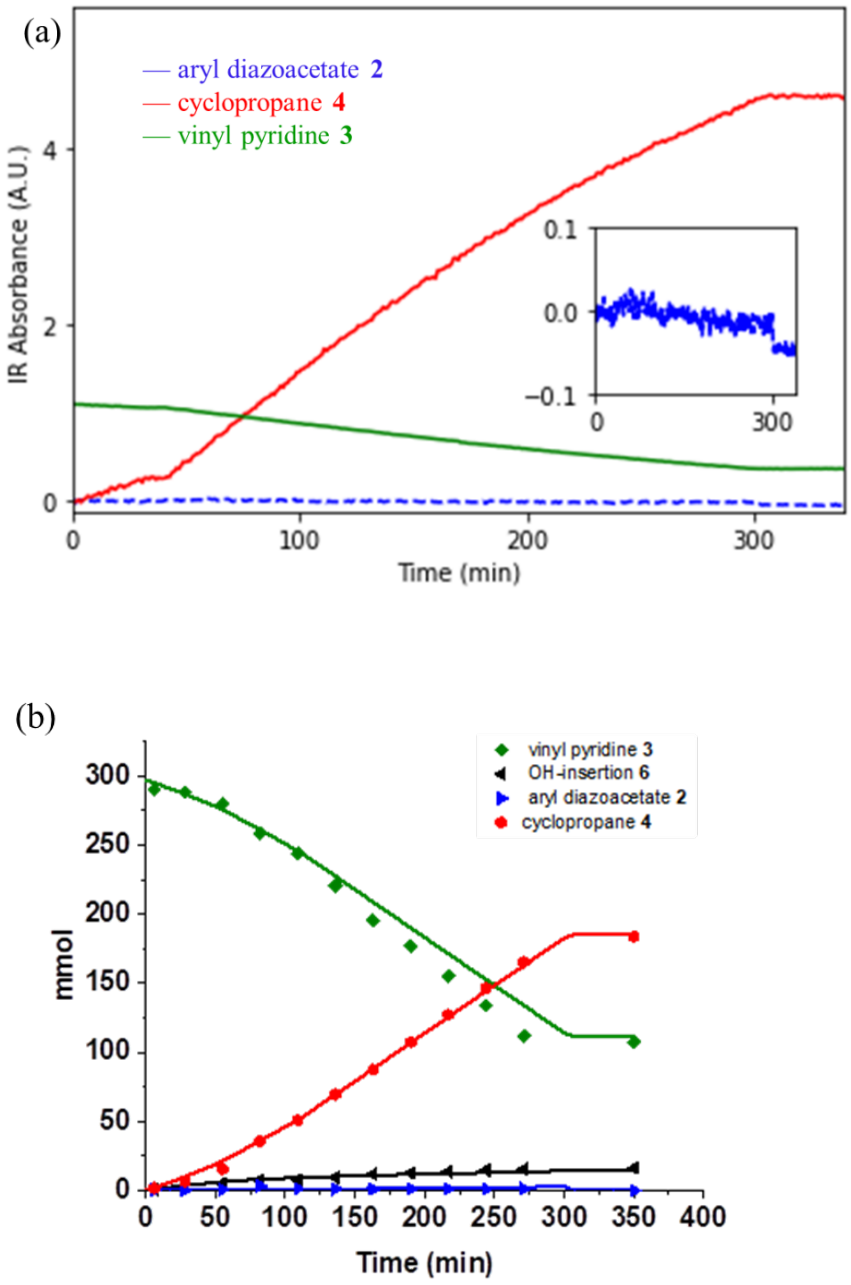

Figure 10 (a) React IR results from fed-batch cyclopropanation **(b)** HPLC results from fed-batch cyclopropanation. Lines represent the fit provided by kinetic deconvolution of the experimental data.[33]

Due to changes in project priorities, further scale-up of cyclopropane **4** was not required; however, encouraged by the success of our 100 g demonstration we concluded this process could

be adapted to support multi-kilogram batches. Lab scale experimentation supported that the design of the PFR, continuous extraction, and molecular sieve drying would scale linearly, with the capability to safely produce cyclopropane **4** at a targeted throughput of 14 kg/day. Consistent with our lab demonstration, react IR would be utilized to monitor the generation of the aryldiazoacetate in the PFR and in the cyclopropanation batch reactor to safeguard against the accumulation of the aryldiazoacetate **2**. Additionally, a quench reactor of phosphoric acid in methanol would be available for the safe quenching of excess diazoacetate generated during start up and shutdown of the process. Importantly, the overall amount of aryldiazoacetate solution at any given time during the continuous process would be ~ 4 L equating to 325 g of aryldiazoacetate **2**.[34] For the preparation of 20 kg of cyclopropane this would represent a 50-fold reduction in aryldiazoacetate generated when compared to a similar batch reaction. The reduction in the amount of aryldiazoacetate coupled with the greatly increased temperature control and heat transfer of a flow reactor compared to a standard jacketed batch reactor highlight the significant safety advantage of conducting this process in flow. This sets the foundation for implementation of this and related chemistries on kilogram scale.

Conclusion

In conclusion, we have successfully developed a safe, continuous flow process for the formation of aryldiazoacetate **2** and its direct use in a sensitive dirhodium-catalyzed asymmetric cyclopropanation reaction. Importantly, the entire process was carried out at reaction temperatures below the decomposition temperature of the diazoacetate intermediate. Following the diazoacetate generation, continuous membrane based aqueous extraction was utilized to efficiently remove the deleterious TMG and mesitylsulfinic acid. Subsequently, molecular sieve column drying provided water levels below 100 ppm in the aryldiazoacetate stream, ensuring

consistent reactivity and selectivity in the sensitive cyclopropanation reaction. The robustness of the cyclopropanation reaction was determined through multivariate and spiking studies to determine acceptable ranges for water content, TMG, mesitylsulfinic acid, 2-fluoropyridine, and HFIP. The full process was successfully demonstrated by processing 100 g of hydrazone **1e** to provide 62.5 g of cyclopropane in 5 h. The tight control of water provided the desired cyclopropane in 74% assay yield, 93 area% purity and 98% ee while limiting the O–H insertion product to 7% assay yield. Furthermore, we have described how this process could be adaptable to further scale up providing throughputs of 14 kg **4**/day. Additionally, we believe the strategy described herein is general and should be adaptable for transformations requiring the safe generation of sensitive aryldiazoacetates and use under "anhydrous" conditions.

EXPERIMENTAL SECTION

General Remarks. Reagents and solvents were used as received without further purification unless stated otherwise. Rh_2(*S*-TPPTTL)$_4$ was prepared according to literature procedure.[2d] NMR spectra were obtained using a Bruker 400 MHz NMR spectrometer. ^{1}H and ^{13}C NMR chemical shifts are expressed in parts per million (δ) relative to the deuterated solvent listed. Purity results reported by HPLC are listed in area percent. Analytical HPLC was performed on an Agilent 1200 HPLC system equipped with UV-DAD detector. The HPLC columns were either Ascentis Express C18 (4.6 mm × 10 cm, 2.7 μm) or Chirapak IC (4.6 mm × 15 cm, 5 μm). DSC data was collected using Mettler Toledo Differential Scanning Calorimeter. ARC data was collected using Netsch Accelerating Rate Calorimeter 254. Heat of reaction data along with gas flow measurements were collected using Omnical SuperCRC (Chemical Reactivity Calorimeter).

Preparation of Tosyl Hydrazone (1a)

A 1 L reactor equipped with overhead stirrer and nitrogen inlet was charged with methyl 2-methoxy-5-methylphenyl)-2-oxoacetate (150 g, 684 mmol, 1 equiv) and methanol (650 mL, 4.3V). Contents of the reactor were adjusted to 30 °C and 4-methylbenzenesulfonohydrazide (134 g, 719 mmol, 1.05 equiv) was added. After 3 h, the slurry was cooled to 0 °C and stirred for 1.5 h. The resulting slurry was filtered and washed with methanol (50 mL, 0.3V). The wet solid was dried in vacuum oven at 50 °C for 20 h to give tosyl hydrazone (**1a**) as a light-yellow solid (224.2 g, 87% yield, 98 area% purity, 50:50 *E/Z* isomers by ^{1}H NMR analysis).

Data for **1a** are as follows. ^{1}H NMR (400 MHz, $CDCl_3$) *50:50 mixture of E/Z isomers:* δ 11.20 (s, 1H), 8.09 (s, 1H), 7.82 (dd, *J* = 8.4, 2.1 Hz, 4H), 7.31 (d, *J* = 8.1 Hz, 2H), 7.26 (d, *J* = 8.1 Hz, 2H), 7.20 (dd, *J* = 8.6, 2.2 Hz, 1H), 7.12 (d, *J* = 8.2 Hz, 2H), 6.88 – 6.79 (m, 2H), 6.73 (d, *J* = 8.1 Hz, 1H), 3.77 (s, 3H), 3.72 (s, 3H), 3.66 (s, 3H), 3.57 (s, 3H), 2.41 (s, 3H), 2.37 (s, 3H),2.26 (s, 3H), 2.25 (s, 3H). ^{13}C NMR (101 MHz, $CDCl_3$) *50:50 mixture of E/Z isomers:* δ 163.89, 162.77, 155.71, 154.03, 144.54, 144.30, 142.56, 138.43, 135.59, 135.28, 132.87, 131.54, 130.96, 130.45, 130.24, 130.04, 129.73, 129.70, 127.93, 127.91, 123.72, 116.76, 111.76, 110.90, 55.77, 55.73, 52.83, 52.52, 21.68, 21.62, 20.43, 20.41. HRMS (LTQ Orbitrap) *m/z* [M +H] calc for $C_{18}H_{20}N_2O_5S$ 377.11657 found 377.11612.

Preparation of Mesitylsulfonyl Hydrazone (1e)

A 1 L reactor equipped with overhead stirrer and nitrogen inlet was charged with methyl 2-methoxy-5-methylphenyl)-2-oxoacetate (75 g, 360 mmol, 1 equiv) and methanol (375 mL, 5V). Contents of the reactor were cooled to 0 °C and 2,4,6-trimethylbenzenesulfonohydrazide (81 g, 378 mmol, 1.05 equiv) was added. After 18 h, the slurry was filtered and washed with methanol (150 mL, 2V). The resulting wet cake was added to 1 L reactor and re-slurried in methanol (200

mL, 2.7V) for 5 h and then filtered and washed with MeOH (150 mL, 2V). The wet solid was dried in vacuum oven at 60 °C for 19 h to give mesitylsulfonyl hydrazone **1e** as a light-yellow solid (109.0 g, 74.8% yield, 97.3 area% purity, 77:23 *E/Z* isomers by ^{1}H NMR analysis).

Data for **1e** are as follows. ^{1}H NMR (400 MHz, Benzene) δ *E isomer*: 9.10 (s, 1H), 7.71 (s, 1H), 7.38 (dd, *J* = 8.4, 2.3 Hz, 1H), 7.16 (s, 2H), 6.91 (d, *J* = 8.5 Hz, 1H), 3.84 (s, 3H), 3.66 (s, 3H), 3.35 (s, 6H), 2.47 (s, 3H), 2.42 (s, 3H). *Z isomer*: 12.59 (s, 1H), 7.75 (s, 1H), 7.38–7.33 (m, 1H), 7.00 (a, 2H), 6.82 (d, *J* = 8.3 Hz, 1H) 3.71 (s, 3H), 3.58 (s, 3H), 3.33 (s, 6H), 2.54 (s, 3H), 2.33 (s, 3H). ^{13}C NMR (101 MHz, Benzene) *E isomer*: 163.83, 154.57, 143.09, 142.01, 140.85, 133.47, 132.19, 130.83, 130.49, 117.70, 111.83, 55.35, 52.04, 23.48, 20.76, 20.23. *Z isomer:* 163.35, 156.15, 142.66, 140.22, 137.71, 133.95, 132.52, 131.27, 130.90, 130.26, 124.69, 111.04, 55.26, 51.86, 23.34, 20.66, 20.24. HRMS (LTQ Orbitrap) *m/z* [M +H] calc for $C_{20}H_{24}N_2O_5S$ 405.14787 found 405.14735.

Batch Preparation of Aryldiazoacetate (2)

A 250 mL round bottom flask equipped with a stir bar was charged with tosyl hydrazone **1a** (5.00 g, 13.28 mmol, 1 equiv) and dichloromethane (100 mL, 20V). The resulting solution was cooled to ~ 0 °C in an ice-water bath and 1,8-diazabicyclo[5.4.0]undec-7-ene (4.04 g, 26.6 mmol, 2.00 equiv) was added over 5 min. The reaction flask was removed from the ice-water bath and allowed to warm to room temperature. After 22 h, reaction mixture was transferred to a separatory funnel and washed with water (2 × 25 mL, 2 × 5V) and 5 wt% aqueous sodium chloride (25 mL, 5V). The resulting organic layer was dried over magnesium sulfate, filtered, and concentrated under reduced pressure. The resulting yellow oil was purified by flash column chromatography on silica gel (eluent: 0%→20% ethyl acetate in hexanes) to afford

aryldiazoacetate (**2)** (2.48 g, 85% yield) as a yellow solid. Spectroscopic data for **2** matched previously measured values.[17]

Preparation of 2-ethoxy-6-vinylpyridine (3)

A 1 L reactor equipped with an overhead stirrer and nitrogen inlet was charged with [1,1'-bis(diphenylphosphino)ferrocene]dichloropalladium(II) (4.35 g, 5.94 mmol, 0.02 equiv) and potassium trifluoro(vinyl)borate (47.7 g, 356 mmol, 1.2 equiv). The reactor was evacuated and back filled with nitrogen 3 times and purged with positive nitrogen pressure for 15 min. A separate flask was charged with 35 wt% aqueous potassium phosphate (114 mL, 356 mmol, 1.2 equiv) and sparged with nitrogen for 45 min. A second flask was charged with 2-bromo-6-ethoxypyridine (60 g, 297 mmol, 1 equiv) and 2-methyl tetrahydrofuran (800 mL, 13.3V) and sparged with nitrogen for 20 min. The reactor was then charged with the degassed solution of 2-bromo-6-ethoxypyridine followed by the degassed solution of aqueous potassium phosphate. The resulting mixture was heated to 70 °C over 30 min. After 11 h, the reaction mixture was cooled to 20 °C and filtered through celite and the reactor was rinsed forward with 2-methyl tetrahydrofuran (180 mL, 3V). The filtrate was collected, and the resulting aqueous layer was separated. The organic layer was washed with water (300 mL, 5V), 12 wt% aqueous 2:1 sodium bicarbonate/cysteine (2 × 300 mL, 2 × 5V), water (300 mL, 5V), 10 wt% aqueous sodium chloride (240 mL, 4V) dried over magnesium sulfate, filtered, and concentrated under reduced pressure. The resulting brown oil was diluted with 2-methyl tetrahydrofuran (500 mL) and concentrated under reduced pressure. This was repeated once more and the resulting crude oil was purified by vacuum distillation at 85 °C and 0.25 torr to give 2-ethoxy-6-vinylpyridine **(3)** as a light-yellow oil (44.3 g, 69.1% yield, 98.6 area% purity, 0.4 wt% water).

Data for **3** are as follows. ^{1}H NMR (400 MHz, DMSO) δ 7.62 (ddd, *J* = 8.2, 7.2, 0.9 Hz, 1H), 6.94 (d, *J* = 7.2 Hz, 1H), 6.70 (dd, *J* = 17.2, 10.5 Hz, 1H), 6.65 (d, *J* = 8.3 Hz, 1H), 6.20 (dd, *J* = 17.3, 2.0 Hz, 1H), 5.38 (dd, *J* = 10.6, 2.0 Hz, 1H), 4.36 – 4.25 (m, 2H), 1.30 (td, *J* = 7.0, 0.9 Hz, 3H).^{13}C NMR (101 MHz, DMSO) δ 162.66, 152.41, 139.47, 136.29, 117.59, 115.01, 110.00, 110.00, 60.70, 14.37. HRMS (LTQ Orbitrap) *m/z* [M +H] calc for $C_9H_{11}NO$ 150.09134 found 150.09129.

Flow Preparation of Aryldiazoacetate (2)

A 500 mL glass bottle was charged with mesitylhydrazone **1e** (140 g, 346 mmol, basis charge) and dichloromethane (462 g, 347 mL, 2.5 V). A second 500 mL glass bottle was charged with 1,1,3,3-tetramethylguanidine (44 g, 382 mmol, 1.1 equiv) and dichloromethane (562 g, 423 mL). Each solution was pumped through a mixing "T" to a PFR, with an inline helical PTFE static mixer (1.7 mm diameter, 17 mm length, containing 10 mixing elements), using a Syrris Asia syringe pump at a flow rate of 1.1 mL/min. The temperature of the PFR (1/8" OD, 657" length, 33 mL volume) was maintained through control of a water bath at 31°C. Post-reaction, water was introduced through a mixing "T" at 2.2 mL/min and mixed with the organic phase using two static mixers (same as above). Continuous extraction was performed using a Zaiput™ membrane extraction system with a 1 μm hydrophobic PTFE membrane. The resulting organic layer was passed through a 2.5 cm diameter glass column packed with 105 g, 3Å molecular sieve (4-8 mesh) operated in up flow. The solution was then passed through React IR flow cell and directly into batch reactor detailed below. Addition of the aryldiazoacetate output stream to cyclopropanation batch reactor described below was started ~45 min after startup.

Fed-Batch Preparation of Cyclopropane (4)

A 500 mL glass bottle was charged with 2-ethoxy-6-vinylpyridine (**3**) (44.3 g, 297 mmol, 1.2 equiv), dichloromethane (200 mL), 1,1,1,3,3,3-hexafluoro-2-propanol (415 g, 2472 mmol, 10 equiv) and 2-fluoropyridine (26.4 g, 272 mmol, 1.1 equiv). The solution was passed through a 2.5 cm diameter glass column packed 3Å molecular sieve (4-8 mesh, 105 g) operated in up flow. The bottle and column were rinsed forward with DCM (300 mL). The resulting dried solution was analyzed for water (133 ppm, 0.034 equiv) by Karl Fisher titrator. The solution was transferred to a 2 L jacketed reactor equipped with an overhead retreat curve impeller and nitrogen inlet. The reactor was charged with Rh_2(*S*-TPPTTL)$_4$ (1.21 g, 0.494 mmol, 0.2 mol%) and 4,4'-di-*tert*-butylbiphenyl (20 g) as HPLC internal standard. The solution was sparged with nitrogen for approximately 15 min and the contents were cooled to an internal temperature of 0 °C. The reactor was equipped with a react IR probe and a Mettler Toledo EZ sampler. The solution of aryldiazoacetate **2** described above was added directly to the batch reactor over a total of 5 h corresponding to 100 g (247 mmol) of mesitylsulfonyl hydrazone **1e** to give cyclopropane **4** (62.5 g, 93 area% purity, 74.3% assay yield, 98% ee).

Data for **4** are as follows. ^{1}H NMR (400 MHz, DMSO) δ 7.41 (dd, *J* = 8.2, 7.3 Hz, 1H), 7.01 (s, 1H), 6.92 – 6.84 (m, 2H), 6.49 (d, *J* = 8.2 Hz, 1H), 6.32 (dd, *J* = 8.2, 0.8 Hz, 1H), 3.78 (dq, *J* = 10.7, 7.0 Hz, 1H), 3.53 (s, 3H), 3.48 (dt, *J* = 10.7, 7.1 Hz, 1H), 3.25 (s, 3H), 3.14 (dd, *J* = 8.8, 6.9 Hz, 1H), 2.21 (dd, *J* = 6.9, 3.9 Hz, 1H), 2.17 (s, 3H), 1.78 (dd, *J* = 8.8, 3.9 Hz, 1H), 1.06 (t, *J* = 7.1 Hz, 3H). ^{13}C NMR (101 MHz, DMSO) δ 173.21, 161.44, 156.39, 153.73, 137.96, 132.42, 128.31, 128.02, 123.73, 116.79, 110.10, 107.30, 60.14, 55.04, 52.06, 33.99, 32.36, 19.92, 19.89, 14.28. HRMS (LTQ Orbitrap) *m/z* [M +H] calc for $C_{20}H_{23}NO_4$ 342.16998 found 342.16915.

ASSOCIATED CONTENT

The Supporting Information is available free of charge at

Experimental procedures and techniques along with representative HPLC traces for reactions and isolated products, ^{1}H and ^{13}C NMR of new compounds, DSC data for all compounds, ARC and Omnical data for aryldiazoacetate and cyclopropane forming reaction mixtures (PDF)

AUTHOR INFORMATION

Corresponding Author

Stephen P. Lathrop - Process Research and Development, AbbVie Inc., North Chicago, Illinois 60064, United States; orcid.org/0000-0002-8375-3993; Email: stephen.lathrop@abbvie.com

Authors

Laurie B. Mlinar - Process Research and Development, AbbVie Inc., North Chicago, Illinois 60064, United States

Onkar N. Manjrekar - Process Research and Development, AbbVie Inc., North Chicago, Illinois 60064, United States

Yong Zhou – Analytical Chemistry, AbbVie Inc., North Chicago, Illinois 60064, United States

Kaid C. Harper - Process Research and Development, AbbVie Inc., North Chicago, Illinois 60064, United States

Eric R. Sacia - Process Research and Development, AbbVie Inc., North Chicago, Illinois 60064, United States

Molly Higgins - Process Research and Development, AbbVie Inc., North Chicago, Illinois 60064, United States

Andrew R. Bogdan – Advanced Chemistry Technologies, AbbVie Inc., North Chicago, Illinois 60064, United States

Zhe Wang - Process Research and Development, AbbVie Inc., North Chicago, Illinois 60064, United States

Steven M. Richter - Process Research and Development, AbbVie Inc., North Chicago, Illinois 60064, United States; orcid.org/0000-0002-5135-9676

Wei Gong – Drug Discovery Science & Technology, AbbVie Inc., North Chicago, Illinois 60064, United States.

Eric A. Voight – Drug Discovery Science & Technology, AbbVie Inc., North Chicago, Illinois 60064, United States.

Jeremy Henle - Process Research and Development, AbbVie Inc., North Chicago, Illinois 60064, United States

Moiz Diwan - Process Research and Development, AbbVie Inc., North Chicago, Illinois 60064, United States

Jeffrey M. Kallemeyn - Process Research and Development, AbbVie Inc., North Chicago, Illinois 60064, United States; orcid.org/0000-0001-7412-360X

Jack C. Sharland – Department of Chemistry, Emory University, 1515 Dickey Drive, Atlanta, Georgia, 30322, United States; orcid.org/0000-0003-0895-6659

Bo Wei - Department of Chemistry, Emory University, 1515 Dickey Drive, Atlanta, Georgia, 30322, United States; orcid.org/0000-0002-6376-6762

Huw M. L. Davies - Department of Chemistry, Emory University, 1515 Dickey Drive, Atlanta, Georgia, 30322, United States; orcid.org/ 0000-0001-6254-9398

Notes

The authors declare the following competing financial interest(s): AbbVie contributed to the design; participated in collection, analysis, and interpretation of data; and in writing, reviewing, and approval of the final version. S.P.L., L.B.M., O.N.M., K.C.H., E.R.S., M.H., A.R.B., Z.W., S.M.R., W.G., E.A.V., J.H., M.D., and J.M.K. are either current or former employees of AbbVie and may own AbbVie stock

ACKNOWLEDGMENT

The work was funded by AbbVie and the National Science Foundation (CHE-1956154). The catalyst used in this study was developed in CCI Center for Selective C–H Functionalization (CHE-1700982).

ABBREVIATIONS

DCM, dichloromethane; DSC, differential scanning calorimetry; ARC, accelerating rate calorimetry; ee, enantiomeric excess; PFR, plug flow reactor; DBU, 1,8-dibiazabicyclo[5.4.0]undec-7-ene; TMG, 1,1,2,2-tetramethylguanidine; BTMG, 2-*tert*-butyl-

1,1,3,3-tetramethylguanidine; IR, infrared; qNMR; quantitative nuclear magnetic resonance; HFIP, 1,1,1,3,3,3-hexafluoro-2-propanol; HPLC, high performance liquid chromatography

REFERENCES

[1] (a) Ye, T.; McKervey, M. A. Organic Synthesis with .Alpha.-Diazo Carbonyl Compounds. *Chem. Rev.* **1994**, *94* (4), 1091–1160. https://doi.org/10.1021/cr00028a010.(b)Ford, A.; Miel, H.; Ring, A.; Slattery, C. N.; Maguire, A. R.; McKervey, M. A. Modern Organic Synthesis with α-Diazocarbonyl Compounds. *Chem. Rev.* **2015**, *115* (18), 9981–10080. https://doi.org/10.1021/acs.chemrev.5b00121.(c) Fructos, M. R.; Díaz-Requejo, M. M.; Pérez, P. J. Gold and Diazo Reagents: A Fruitful Tool for Developing Molecular Complexity. *Chem. Commun.* **2016**, *52* (46), 7326–7335. https://doi.org/10.1039/C6CC01958G. (d) Mix, K. A.; Aronoff, M. R.; Raines, R. T. Diazo Compounds: Versatile Tools for Chemical Biology. *ACS Chem. Biol.* **2016**, *11* (12), 3233–3244. https://doi.org/10.1021/acschembio.6b00810.(e) Ciszewski, Ł. W.; Rybicka-Jasińska, K.; Gryko, D. Recent Developments in Photochemical Reactions of Diazo Compounds. *Org. Biomol. Chem.* **2019**, *17* (3), 432–448. https://doi.org/10.1039/C8OB02703J.

[2] Selected C-H insertion examples: (a) Demonceau, A.; Noels, A. F.; Hubert, A. J.; Teyssié, P. Transition-Metal-Catalysed Reactions of Diazoesters. Insertion into C–H Bonds of Paraffins by Carbenoids. *J. Chem. Soc., Chem. Commun.* **1981**, No. 14, 688–689. https://doi.org/10.1039/C39810000688. (b) Davies, H. M. L.; Hansen, T.; Churchill, M. R. Catalytic Asymmetric C–H Activation of Alkanes and Tetrahydrofuran. *J. Am. Chem. Soc.* **2000**, *122* (13), 3063–3070. https://doi.org/10.1021/ja994136c. (c) Davies, H. M. L.; Grazini, M. V. A.; Aouad, E. Asymmetric Intramolecular C–H Insertions of Aryldiazoacetates. *Org. Lett.* **2001**, *3* (10), 1475–1477. https://doi.org/10.1021/ol0157858. (d) Fu, J.; Ren, Z.; Bacsa, J.; Musaev, D. G.; Davies, H. M. L. Desymmetrization of Cyclohexanes by Site- and Stereoselective C–H Functionalization. *Nature* **2018**, *564* (7736), 395–399. https://doi.org/10.1038/s41586-018-0799-2. Selected C-H insertion reviews: (e) Davies, H. M. L.; Beckwith, R. E. J. Catalytic Enantioselective C–H Activation by Means of Metal–Carbenoid-Induced C–H Insertion. *Chem. Rev.* **2003**, *103* (8), 2861–2904. https://doi.org/10.1021/cr0200217. (f) Davies, H. M. L.; Manning, J. R. Catalytic C–H Functionalization by Metal Carbenoid and Nitrenoid Insertion. *Nature* **2008**, *451* (7177), 417–424. https://doi.org/10.1038/nature06485.(g) Davies, H. M. L.; Morton, D. Guiding Principles for Site Selective and Stereoselective Intermolecular C–H Functionalization by Donor/Acceptor Rhodium Carbenes. *Chem. Soc. Rev.* **2011**, *40* (4), 1857–1869. https://doi.org/10.1039/C0CS00217H. (h) Xia, Y.; Qiu, D.; Wang, J. Transition-Metal-Catalyzed Cross-Couplings through Carbene Migratory Insertion. *Chem. Rev.* **2017**, *117* (23), 13810–13889. https://doi.org/10.1021/acs.chemrev.7b00382. (i) Davies, H. M. L.; Liao, K. Dirhodium Tetracarboxylates as Catalysts for Selective Intermolecular C–H Functionalization. *Nat. Rev. Chem.* **2019**, *3* (6), 347–360. https://doi.org/10.1038/s41570-019-0099-x.

[3] Selected N-H insertion examples: (a) Karady, S.; Amato, J. S.; Reamer, R. A.; Weinstock, L. M. Stereospecific Conversion of Penicillin to Thienamycin. *J. Am. Chem. Soc.* **1981**, *103* (22), 6765–6767. https://doi.org/10.1021/ja00412a048. (b) Xu, B.; Zhu, S.-F.; Xie, X.-L.; Shen, J.-J.; Zhou, Q.-L. Asymmetric N H Insertion Reaction Cooperatively Catalyzed by Rhodium and Chiral Spiro Phosphoric Acids. *Angew. Chem., Int. Ed.* **2011**, *50* (48), 11483–11486. https://doi.org/10.1002/anie.201105485. (c) Nicolle, S. M.; Lewis, W.; Hayes, C. J.; Moody, C. J. Stereoselective Synthesis of Functionalized Pyrrolidines by the Diverted N–H Insertion Reaction of Metallocarbenes with β-Aminoketone Derivatives. *Angew. Chem., Int. Ed.* **2016**, *55* (11), 3749–3753. https://doi.org/10.1002/anie.201511433. (d) Boddy, A. J.; Affron, D. P.; Cordier, C. J.; Rivers, E. L.; Spivey, A. C.; Bull, J. A. Rapid Assembly of Saturated Nitrogen Heterocycles in One-Pot: Diazo-Heterocycle "Stitching" by N–H Insertion and Cyclization. *Angew. Chem., Int. Ed.* **2019**, *58* (5), 1458–1462. https://doi.org/10.1002/anie.201812925. (e) Ratcliffe, R. W. Salzmann, T. N.; Christensen, B. G. A Novel Synthesis Of The Carbapen-2-em Ring System *Tetrahedron Lett.* **1980**, 31-34.

[4] Selcted O-H insertion example: (a) Davis, O. A.; Bull, J. A. Synthesis of Di-, Tri-, and Tetrasubstituted Oxetanes by Rhodium-Catalyzed O-H Insertion and C-C Bond-Forming Cyclization. *Angew. Chem., Int. Ed.* **2014**, *53* (51), 14230–14234. https://doi.org/10.1002/anie.201408928. (b) Davis, O. A.; Croft, R. A.; Bull, J. A. Synthesis of

Diversely Functionalised 2,2-Disubstituted Oxetanes: Fragment Motifs in New Chemical Space. *Chem. Commun.* **2015**, *51* (84), 15446–15449. https://doi.org/10.1039/C5CC05740J. (c) Nicolle, S. M.; Lewis, W.; Hayes, C. J.; Moody, C. J. Stereoselective Synthesis of Highly Substituted Tetrahydrofurans through Diverted Carbene O-H Insertion Reaction. *Angew. Chem., Int. Ed.* **2015**, *54* (29), 8485–8489. https://doi.org/10.1002/anie.201502484. (d)Davis, O. A.; Croft, R. A.; Bull, J. A. Synthesis of Substituted 1,4-Dioxenes through O–H Insertion and Cyclization Using Keto-Diazo Compounds. *J. Org. Chem.* **2016**, *81* (22), 11477–11488. https://doi.org/10.1021/acs.joc.6b02134.

[5] (a) Selected S-H, P-H and Si-H insertion examples: Bartrum, H. E.; Blakemore, D. C.; Moody, C. J.; Hayes, C. J. Continuous-Flow Generation of Diazoesters and Their Direct Use in S–H and P–H Insertion Reactions: Synthesis of α-Sulfanyl, α-Sulfonyl, and α-Phosphono Carboxylates. *Tetrahedron* **2013**, *69* (10), 2276–2282. https://doi.org/10.1016/j.tet.2013.01.020. (b) Keipour, H.; Jalba, A.; Delage-Laurin, L.; Ollevier, T. Copper-Catalyzed Carbenoid Insertion Reactions of α-Diazoesters and α-Diazoketones into Si–H and S–H Bonds. *J. Org. Chem.* **2017**, *82* (6), 3000–3010. https://doi.org/10.1021/acs.joc.6b02998.

[6] Selected cyclopropanation reviews: Lebel, H.; Marcoux, J.-F.; Molinaro, C.; Charette, A. B. Stereoselective Cyclopropanation Reactions. *Chem. Rev.* **2003**, *103* (4), 977–1050. https://doi.org/10.1021/cr010007e. (b) Maas, G. Ruthenium-Catalysed Carbenoid Cyclopropanation Reactions with Diazo Compounds. *Chem. Soc. Rev.* **2004**, *33* (3), 183–190. https://doi.org/10.1039/B309046A. (c) Davies, H. M. L.; Antoulinakis, E. G. Intermolecular Metal-Catalyzed Carbenoid Cyclopropanation. *Organic Reactions;* John Wiley & Sons, Ltd.: Hoboken, NJ, 2001; Vol. *57*, 1-326.

[7] (a) Aggarwal, V. K.; de Vicente, J.; Bonnert, R. V. A Novel One-Pot Method for the Preparation of Pyrazoles by 1,3-Dipolar Cycloadditions of Diazo Compounds Generated in Situ. *J. Org. Chem.* **2003**, *68* (13), 5381–5383. https://doi.org/10.1021/jo0268409. (b) Babinski, D. J.; Aguilar, H. R.; Still, R.; Frantz, D. E. Synthesis of Substituted Pyrazoles via Tandem Cross-Coupling/Electrocyclization of Enol Triflates and Diazoacetates. *J. Org. Chem.* **2011**, *76* (15), 5915–5923. https://doi.org/10.1021/jo201042c. (c) Wu, L.-L.; Ge, Y.-C.; He, T.; Zhang, L.; Fu, X.-L.; Fu, H.-Y.; Chen, H.; Li, R.-X. An Efficient One-Pot Synthesis of 3,5-Disubstituted 1H-Pyrazoles. *Synthesis* **2012**, *44* (10), 1577–1583. https://doi.org/10.1055/s-0031-1290772. (d) Mykhailiuk, P. K.; Ishchenko, A. Y.; Stepanenko, V.; Cossy, J. Synthesis of Fluoroalkyl Pyrazoles from In-Situ-Generated C2F5CHN2 and Electron-Deficient Alkenes. *Eur. J. Org. Chem.* **2016**, *2016* (33), 5485–5493. https://doi.org/10.1002/ejoc.201600947. (e) Zhang, B.; Davies, H. M. L. Rhodium-Catalyzed Enantioselective [4+2] Cycloadditions of Vinylcarbenes with Dienes. *Angew. Chem. Int. Ed.* **2020**, *59* , 4937–4941. https://doi.org/10.1002/ange.201914354.

[8] Simpson, J. H.; Kotnis, A. S.; Deshpande, R. P.; Kacsur, D. J.; Hamm, J.; Kodersha, G.; Merkl, W.; Domina, D.; Wang, S. Y. Development of a Multi-Kilogram Procedure to Prepare, Use, and Quench Ethyl Diazoaceate. In *Managing Hazardous Reactions and Compounds in Process Chemistry;* Pesti, J. A.; Abdel-Magid, A. F., Eds.; America Chemical Society: Washington DC, 2014; Chapter 9, 235-244.

[9] Green, S. P.; Wheelhouse, K. M.; Payne, A. D.; Hallett, J. P.; Miller, P. W.; Bull, J. A. Thermal Stability and Explosive Hazard Assessment of Diazo Compounds and Diazo Transfer Reagents. *Org. Process Res. Dev.* **2020**, *24* (1), 67–84. https://doi.org/10.1021/acs.oprd.9b00422.

[10] (a) Anthes, R.; Bello, O.; Benoit, S.; Chen, C.-K.; Corbett, E.; Corbett, R. M.; DelMonte, A. J.; Gingras, S.; Livingston, R.; Sausker, J.; Soumeillant, M. Kilogram Synthesis of a Selective Serotonin Reuptake Inhibitor. *Org. Process Res. Dev.* **2008**, *12* (2), 168–177. https://doi.org/10.1021/op700125z. (b) Bien, J.; Davulcu, A.; DelMonte, A. J.; Fraunhoffer, K. J.; Gao, Z.; Hang, C.; Hsiao, Y.; Hu, W.; Katipally, K.; Littke, A.; Pedro, A.; Qiu, Y.; Sandoval, M.; Schild, R.; Soltani, M.; Tedesco, A.; Vanyo, D.; Vemishetti, P.; Waltermire, R. E. The First Kilogram Synthesis of Beclabuvir, an HCV NS5B Polymerase Inhibitor. *Org. Process Res. Dev.* **2018**, *22* (10), 1393–1408. https://doi.org/10.1021/acs.oprd.8b00214. (c) Gage, J. R.; Chen, F.; Dong, C.; Gonzalez, M. A.; Jiang, Y.; Luo, Y.; McLaws, M. D.; Tao, J. Semicontinuous Process for GMP Manufacture of a Carbapenem Intermediate via Carbene Insertion Using an Immobilized Rhodium Catalyst. *Org. Process Res. Dev.* **2020**, *24* (10), 2025–2033. https://doi.org/10.1021/acs.oprd.0c00133.

[11] Clark, J. D.; Shah, A. S.; Peterson, J. C. Understanding the Large-Scale Chemistry of Ethyl Diazoacetate via Reaction Calorimetry. *Thermochimica Acta* **2002**, *392–393*, 177–186. https://doi.org/10.1016/S0040-6031(02)00100-4.

[12] Hock, K. J.; Koenigs, R. M. The Generation of Diazo Compounds in Continuous-Flow. *Chemistry - A European Journal* **2018**, *24* (42), 10571–10583. https://doi.org/10.1002/chem.201800136.

[13] (a) Nicolle, S. M.; Hayes, C. J.; Moody, C. J. Alkyl Halide-Free Heteroatom Alkylation and Epoxidation Facilitated by a Recyclable Polymer-Supported Oxidant for the In-Flow Preparation of Diazo Compounds. *Chem. - Eur. J.* **2015**, *21* (12), 4576–4579. https://doi.org/10.1002/chem.201500118. (b) Poh, J.-S.; Tran, D. N.; Battilocchio, C.; Hawkins, J. M.; Ley, S. V. A Versatile Room-Temperature Route to Di- and Trisubstituted Allenes Using Flow-Generated Diazo Compounds. *Angew. Chem., Int. Ed.* **2015**, *54* (27), 7920–7923. https://doi.org/10.1002/anie.201501538.(c) Roda, N. M.; Tran, D. N.; Battilocchio, C.; Labes, R.; Ingham, R. J.; Hawkins, J. M.; Ley, S. V. Cyclopropanation Using Flow-Generated Diazo Compounds. *Org. Biomol. Chem.* **2015**, *13* (9), 2550–2554. https://doi.org/10.1039/C5OB00019J.(d) Tran, D. N.; Battilocchio, C.; Lou, S.-B.; Hawkins, J. M.; Ley, S. V. Flow Chemistry as a Discovery Tool to Access Sp2–Sp3 Cross-Coupling Reactions via Diazo Compounds. *Chem. Sci.* **2015**, *6* (2), 1120–1125. https://doi.org/10.1039/C4SC03072A. (e)
Poh, J.-S.; Makai, S.; von Keutz, T.; Tran, D. N.; Battilocchio, C.; Pasau, P.; Ley, S. V. Rapid Asymmetric Synthesis of Disubstituted Allenes by Coupling of Flow-Generated Diazo Compounds and Propargylated Amines. *Angew. Chem., Int. Ed.* **2017**, *56* (7), 1864–1868. https://doi.org/10.1002/anie.201611067. (f) Rackl, D.; Yoo, C.-J.; Jones, C. W.; Davies, H. M. L. Synthesis of Donor/Acceptor-Substituted Diazo Compounds in Flow and Their Application in Enantioselective Dirhodium-Catalyzed Cyclopropanation and C–H Functionalization. *Org. Lett.* **2017**, *19* (12), 3055–3058. https://doi.org/10.1021/acs.orglett.7b01073. (g) Yoo, C.-J.; Rackl, D.; Liu, W.; Hoyt, C. B.; Pimentel, B.; Lively, R. P.; Davies, H. M. L.; Jones, C. W. An Immobilized-Dirhodium Hollow-Fiber Flow Reactor for Scalable and Sustainable C–H Functionalization in Continuous Flow. *Angew. Chem., Int. Ed.* **2018**, *57* (34), 10923–10927. https://doi.org/10.1002/anie.201805528. (h) Wei, B.; Hatridge, T. A.; Jones, C. W.; Davies, H. M. L. Copper(II) Acetate-Induced Oxidation of Hydrazones to Diazo Compounds under Flow Conditions Followed by Dirhodium-Catalyzed Enantioselective Cyclopropanation Reactions. *Org. Lett.* **2021**, *23* (14), 5363–5367. https://doi.org/10.1021/acs.orglett.1c01580. (i) Hatridge, T. A.; Wei, B.; Davies, H. M. L.; Jones, C. W. Copper-Catalyzed, Aerobic Oxidation of Hydrazone in a Three-Phase Packed Bed Reactor. *Org. Process Res. Dev.* **2021**, *25* (8), 1911–1922. https://doi.org/10.1021/acs.oprd.1c00165.

[14] (a) Müller, S. T. R.; Murat, A.; Maillos, D.; Lesimple, P.; Hellier, P.; Wirth, T. Rapid Generation and Safe Use of Carbenes Enabled by a Novel Flow Protocol with In-Line IR Spectroscopy. *Chem. – Eur. J.* **2015**, *21* (19), 7016–7020. https://doi.org/10.1002/chem.201500416. (b) Deadman, B. J.; O'Mahony, R. M.; Lynch, D.; Crowley, D. C.; Collins, S. G.; Maguire, A. R. Taming Tosyl Azide: The Development of a Scalable Continuous Diazo Transfer Process. *Org. Biomol. Chem.* **2016**, *14* (13), 3423–3431. https://doi.org/10.1039/C6OB00246C.
(c) Müller, S. T. R.; Murat, A.; Hellier, P.; Wirth, T. Toward a Large-Scale Approach to Milnacipran Analogues Using Diazo Compounds in Flow Chemistry. *Org. Process Res. Dev.* **2016**, *20* (2), 495–502. https://doi.org/10.1021/acs.oprd.5b00308. (d) O'Mahony, R. M.; Lynch, D.; O'Callaghan, K. S.; Collins, S. G.; Maguire, A. R. Generation of Tosyl Azide in Continuous Flow Using an Azide Resin, and Telescoping with Diazo Transfer and Rhodium Acetate-Catalyzed O–H Insertion. *Org. Process Res. Dev.* **2021**. https://doi.org/10.1021/acs.oprd.1c00377.

[15] (a) Bartrum, H. E.; Blakemore, D. C.; Moody, C. J.; Hayes, C. J. Rapid Access to α-Alkoxy and α-Amino Acid Derivatives through Safe Continuous-Flow Generation of Diazoesters. *Chem. – Eur. J.* **2011**, *17* (35), 9586–9589. https://doi.org/10.1002/chem.201101590. (b) Bartrum, H. E.; Blakemore, D. C.; Moody, C. J.; Hayes, C. J. Continuous-Flow Generation of Diazoesters and Their Direct Use in S–H and P–H Insertion Reactions: Synthesis of α-Sulfanyl, α-Sulfonyl, and α-Phosphono Carboxylates. *Tetrahedron* **2013**, *69* (10), 2276–2282. https://doi.org/10.1016/j.tet.2013.01.020.

[16] TsN_3 has T_{init} = 128 ° C and T_{onset} = 158 ° C, *p*-ABSA T_{init} = 120-130 ° C and T_{onset} = 138-136 ° C (Ref 9). This can be directly compared to tosyl hydrazone **1a**: T_{init} = 129 ° C and T_{onset} = 205 ° C and mesitylsulfonyl hydrazone **1e** T_{init} = 151 ° C and T_{onset} = 182 ° C see supporting information for more details.

[17] Sharland, J. C.; Wei, B.; Hardee, D. J.; Hodges, T. R.; Gong, W.; Voight, E. A.; Davies, H. M. L. Asymmetric Synthesis of Pharmaceutically Relevant 1-Aryl-2-Heteroaryl- and 1,2-Diheteroarylcyclopropane-1-Carboxylates. *Chem. Sci.* **2021**, *12* (33), 11181–11190. https://doi.org/10.1039/D1SC02474D.

[18] T_{init} is used here to describe initiation temperature in DSC samples consistent with ref 9. T_{onest} is used to describe onset temperatures observed in ARC studies

[19] Stoessel, I. F. *Thermal Safety of Chemical Processes: Risk Assessment and Process Design*; Wiley-VCH Verlag GmbH & Co. KGaA, 2008.
[20] Sperry, J. B.; Minteer, C. J.; Tao, J. Y.; Johnson, R.; Duzguner, R.; Hawksworth, M.; Oke, S.; Richardson, P. F.; Barnhart, R.; Bill, D. R.; Giusto, R. A.; Weaver, J. D. Thermal Stability Assessment of Peptide Coupling Reagents Commonly Used in Pharmaceutical Manufacturing. *Org. Process Res. Dev.* **2018**, *22*, 1262-1275. https://doi.org/10.1021/acs.oprd.8b00193.
[21] Levin, D. Managing Hazards for Scale Up of Chemical Manufacturing Processes. In *Managing Hazardous Reactions and Compounds in Process Chemistry*; Pesti, J.A. and Abdel-Magid, A.F., Eds; Oxford University Press, 2014; pp 3-71.
[22] Hydrazone starting materials were isolated and used in the Bamford-Stevens reaction as a mixture of *E*/*Z* isomers around the N-N bond. Structural assignment of the *E*/*Z* isomers was based on comparison of the ^{1}H NMR with computational predictions (see Supporting Information for details).
[23] Dudman, C. D.; Reese, C. B. Preparation of Aryldiazoalkanes from 2,4,6-Triisopropylbenzenesulphonyl Hydrazones. *Synthesis* **1982**, *5*, 419–421.
[24] (a) Nelson, T. D.; Song, Z. J.; Thompson, A. S.; Zhao, M.; DeMarco, A.; Reamer, R. A.; Huntington, M. F.; Grabowski, E. J. .; Reider, P. J. Rhodium-Carbenoid-Mediated Intermolecular O–H Insertion Reactions: A Dramatic Additive Effect. Application in the Synthesis of an Ascomycin Derivative. *Tetrahedron Lett.* **2000**, *41* (12), 1877–1881. https://doi.org/10.1016/S0040-4039(00)00069-1. (b) Ye, Q.-S.; Li, X.-N.; Jin, Y.; Yu, J.; Chang, Q.-W.; Jiang, J.; Yan, C.-X.; Li, J.; Liu, W.-P. Synthesis, Crystal Structures and Catalytic Activity of Tetrakis(Acetato)Dirhodium(II) Complexes with Axial Picoline Ligands. *Inorg. Chim. Acta* **2015**, *434*, 113–120. https://doi.org/10.1016/j.ica.2015.05.017.
[25] (a) Weeranoppanant, N.; Adamo, A.; Saparbaiuly, G.; Rose, E.; Fleury, C.; Schenkel, B.; Jensen, K. F. Design of Multistage Counter-Current Liquid–Liquid Extraction for Small-Scale Applications. *Ind. Eng. Chem. Res.* **2017**, *56* (14), 4095–4103. https://doi.org/10.1021/acs.iecr.7b00434.
(b) Weeranoppanant, N.; Adamo, A. In-Line Purification: A Key Component to Facilitate Drug Synthesis and Process Development in Medicinal Chemistry. *ACS Med. Chem. Lett.* **2020**, *11* (1), 9–15. https://doi.org/10.1021/acsmedchemlett.9b00491.
[26] see supplementary information for details.
[27] Although, conducting the cyclopropanation in flow was also considered, the nitrogen gas evolution during the cyclopropanation step precluded the use of a PFR and the simpler approach of a fed-batch process was pursued.
[28] Williams, D. B. G.; Lawton, M. Drying of Organic Solvents: Quantitative Evaluation of the Efficiency of Several Desiccants. *J. Org. Chem.* **2010**, *75* (24), 8351–8354. https://doi.org/10.1021/jo101589h.
[29] For a discussion on the role of pyridine additive in cyclopropanation reaction, see ref 17. **Error! Bookmark not defined.**
[30] Claxton, L. D.; Dearfield, K. L.; Spanggord, R. J.; Riccio, E. S.; Mortelmans, K. Comparative Mutagenicity of Halogenated Pyridines in the Salmonella Typhimurium/Mammalian Microsome Test. *Mutat. Res., Fundam. Mol. Mech. Mutagen.* **1987**, *176* (2), 185–198. https://doi.org/10.1016/0027-5107(87)90049-2.
[31] During extraction, there was a brief downtime to change the equipment due to the observation of inefficient aqueous/organic separation via the membrane separator. The poor separation resulted in increased loss of the aryldiazoacetate **2** to the aqueous waste corresponding in a delay in reaching the expected steady state concentration. Due to material limitations, aryldiazoacetate solution was diverted to the cyclopropanation reaction prior to fully reaching steady state.
[32] A delay in reaching steady state in the aryldiazoacetate PFR (see ref 31) resulted in slightly lower yield of cyclopropane **4** than anticipated. For example, the assay yield of cyclopropanation reaction while the PFR was operating at steady state (between 163-271 min) was 86%.
[33] See supporting information for details.
[34] For this calculation we used a hypothetical PFR using 48.2 ft of ½" PTFE tubing at a total flow rate of 100 mL/min and 15 cm diameter × 55 cm length stainless steel molecular sieve column with 26% void space.